

Body condition as a shared response to environment in a  
commercially important demersal fish assemblage

Philina A. English<sup>1</sup>, Sean C. Anderson<sup>1,2</sup>, and Robyn E. Forrest<sup>1</sup>

<sup>1</sup>Pacific Biological Station, Fisheries and Oceans Canada, Nanaimo, BC, Canada

<sup>2</sup>School of Resource and Environmental Management, Simon Fraser University,  
Burnaby, BC, Canada

\*corresponding author: [ecophilina@gmail.com](mailto:ecophilina@gmail.com)

**Short running head:** Body condition as a shared response

## Abstract

Measures of an organism's weight at a given length are often considered reliable indicators of energy reserves or 'condition', which can be related to fecundity and risk of mortality. Understanding the impact of environmental change on fish condition may therefore be critical for sustainable management of human activities in marine ecosystems. We investigated how changes in Canadian Pacific waters may be influencing average condition of 35 commercially, culturally, or ecologically important demersal fish species. Because condition of mature male and female, and immature individuals have different implications for population dynamics, ecological drivers, and measurement, we separated individual fish and overall catches into these components, then estimated density distributions, calculated Le Cren's relative body condition deviations, modelled spatiotemporal change in these deviations, and generated density-weighted annual indices of body condition. We then used Bayesian Dynamic Factor Analysis to identify common trends across species and tested for correlations with environmental variables. For most species, warmer sea surface temperature and lagged North Pacific Gyre Oscillation appeared neutrally or positively correlated with condition. Only immature condition was also strongly correlated with primary production, but this effect was equally likely to be negative (e.g., Pacific Spiny Dogfish, Lingcod, Sablefish) as positive (e.g., Quillback Rockfish, Southern Rock Sole, Spotted Ratfish). Our approach propagates uncertainty from condition estimation through to environmental correlations and provides both an ecosystem perspective as well as species-specific inference. Robust estimates of relationships between condition and environmental variables can inform ecosystem approaches to fisheries management including short-term forecasts of weight-at-age or recruitment.

**Keywords:** Le Cren's body condition, spatiotemporal modelling, Bayesian Dynamic Factor analysis, groundfish, ecosystem-based fisheries management, climate change

# Contents

<b>Contents</b>	<b>3</b>
<b>1 Introduction</b>	<b>4</b>
<b>2 Methods</b>	<b>7</b>
2.1 Splitting specimens and total catch by sex and maturity . . . . .	7
2.2 Spatiotemporal estimates of biomass density . . . . .	9
2.3 Body condition index . . . . .	11
2.4 Identify common trends . . . . .	13
2.5 Test for environmental correlates . . . . .	14
<b>3 Results</b>	<b>16</b>
3.1 Sex and maturity specific biomass indices . . . . .	16
3.2 Body condition indices . . . . .	17
3.3 Environmental correlates of body condition . . . . .	17
<b>4 Discussion</b>	<b>19</b>
<b>5 Acknowledgements</b>	<b>24</b>
<b>6 Data availability statement</b>	<b>24</b>
<b>7 Conflict of Interest</b>	<b>24</b>
<b>8 Bibliography</b>	<b>25</b>
<b>9 Figures</b>	<b>33</b>

# 1 Introduction

Uncertainty arising from climate-related changes in the ocean creates challenges for management of fisheries, where best practice requires management of risk to ensure sustainable harvests and maintenance of healthy ecosystems (Francis and Shotton 1997, Roux *et al.* 2022). Increasingly, legislation and policy around the world, including in Canada, the USA, Europe, Australia and New Zealand, call for an ecosystem approach to the management of fisheries, where environmental considerations are accounted for in management decisions (Marentette and Kronlund 2020). While environmental variables have been linked to productivity variables such as recruitment (Haltuch *et al.* 2019, Maunder and Thorson 2019), growth (Whitten *et al.* 2013, Stawitz *et al.* 2019) and survival (Johnson *et al.* 2015, Legault and Palmer 2015, Punt *et al.* 2021), quantitative application of these links in fishery stock assessment and decision-making contexts remains relatively rare due to the large uncertainties in mechanistic links between specific environmental variables and biological processes (e.g., Pepin *et al.* 2022). Such uncertainties can result from complexity, confounding factors, and/or limited data at the appropriate spatial and temporal scales (Punt *et al.* 2014). Furthermore, even when relationships between environmental variables and biological processes such as recruitment have been established, they are prone to break down over time, especially in the presence of large scale environmental change, making prediction difficult or even risk-prone (Myers *et al.* 1995, Myers 1998, Tamburello *et al.* 2019).

Large-scale changes in environmental conditions such as those caused by global climate change can impact marine fish populations at multiple scales, potentially magnifying natural fluctuations or causing trends in population size and productivity through altered growth, reproductive capacity, survival, and/or distribution (Szuwalski and Hollowed 2016, Free *et al.* 2019, Bryndum-Buchholz *et al.* 2020). Warming ocean conditions, leading to changes in ocean circulation and stratification, oxygen concentration, and primary productivity, can directly impact the physiology and behaviour of individual animals, as well as the productivity (Free *et al.* 2019) and composition of the surrounding ecosystem that can influence prey availability (Evans *et al.* 2023), susceptibility to predation, and habitat suitability (Brander 2007, Boudreau *et al.* 2015).

Body condition, essentially a measure of a fish's weight relative to its length, reflects the ability of an individual or population of fish to find and store energy under prevailing environmental conditions and, as such, may be a useful indicator of future reproduction and survival success that integrates ecosystem effects such as diet, habitat, and temperature but doesn't depend on understanding

mechanistic relationships between environmental variables and specific biological processes (Dutil *et al.* 1995, Boldt and Rooper 2009). While there are many approaches to calculating condition from length and somatic weight, or other metrics such as gonads, muscle, or liver dry weight or energy content (Dutil *et al.* 1995, Dutil and Lambert 2000, Peig and Green 2010), Le Cren's relative condition (Le Cren 1951), which uses the length-weight parameters for a population to calculate the expected weight, is currently the most widely used in fisheries studies (Gubiani *et al.* 2020). Of the methods that require only length and somatic weight, Le Cren's avoids size bias and showed greatest consistency across species making it most suitable for multispecies and ecosystem analyses (Wuenschel *et al.* 2019).

Body condition is often related to the main productivity variables of growth, reproduction and survival (Gubiani *et al.* 2020). A recent study of eleven North Sea fish stocks found that average weight of spawners was positively correlated with recruitment anomalies in the majority of the stocks, and that average weight of spawners was a better predictor of recruitment than either the proportion of old spawners in the population or the average age of spawners (Van Deurs *et al.* 2023). Other studies have also reported positive correlations between body condition and recruitment, e.g., for haddock (Friedland *et al.* 2015), juvenile Bering Sea pollock (Heintz *et al.* 2013) and Atlantic cod (Rätz and Lloret 2003). Other studies on Atlantic cod have found significant relationships between body condition and natural mortality, both under laboratory conditions (Dutil and Lambert 2000) and in wild populations, where poor condition has been a key factor in failure of stocks to recover from low population size (Dutil *et al.* 1995, Casini *et al.* 2016a, Regular *et al.* 2022). Proposed mechanisms for lower survival rates in fish with poor body condition include greater susceptibility to starvation, disease and vulnerability to fishing gear (Dutil *et al.* 1995, Casini *et al.* 2016a). Fish in poor condition may also have a lower probability of being mature (Morgan 2004). Changes in average body condition may therefore provide an early indication of likely impacts to population productivity that are not captured in more commonly reported population metrics such as spawning biomass. Since body condition is relatively cheap to measure, reporting body condition indices as an additional biological metric in stock assessment advice would provide one means of considering implicit effects of ecosystem processes in decision-making without the need to fully understand mechanistic links between specific environmental variables and biological processes (Dutil *et al.* 1995, Casini *et al.* 2016a, Regular *et al.* 2022, Van Deurs *et al.* 2023).

The nutrient-rich waters along the Pacific coast of British Columbia, Canada, support an economically, culturally, and ecologically important community of benthic fish species (hereafter, ground-

fish). Collectively, these species occupy a large range of habitats and depths, exhibit varying degrees of philopatry (Love 2011), and vary in longevity, growth rates (Anderson *et al.* 2019) and physiological tolerances (Keller *et al.* 2017). While many species are projected to shift to deeper depths as conditions warm (Dulvy *et al.* 2008, Pinsky *et al.* 2013), low oxygen will limit how deep they can go (Thompson *et al.* 2023). Furthermore, a warmer ocean is expected become more stratified and hold less oxygen (Levin and Le Bris 2015). Indeed, previous work has shown a range of both positive and negative abundance and distribution changes in response to ocean temperature and oxygen availability by species in this assemblage (English *et al.* 2021, Thompson *et al.* 2023). Shifts in distribution and abundance can be particularly challenging for management of multispecies fisheries, such as trawl and longline fisheries, where the ability to selectively target or avoid species is limited and when species redistribution causes novel species ratios and mixes. As a result, a better understanding of both assemblage and species-level responses to environmental conditions will be increasingly critical for effective management of these fisheries.

Because body condition reflects both the shared environmental and ecosystem conditions, as well as individual diet, metabolism, and physiological tolerance, there is the potential for both synchrony and contrasting effects among species, maturity classes, and sexes. To better understand these effects, we developed a multi-species, sex- and maturity-disaggregated framework for generating annual indices of average body condition for the 35 Pacific Canadian groundfish species for which we had sufficient data. Analyses were applied to each portion of a species' population, defined as mature male, mature female and immature (species-level analysis in Figure 1). We then used a Bayesian implementation of a Dynamic Factor Analysis (DFA; Ward *et al.* 2019) to identify: 1) common trends and contrasting effects across species within each sex and maturity class; and 2) potential environmental correlates of these assemblage-level patterns (ecosystem-level analysis in Figure 1). For all sex and maturity classes, we found that sea surface temperature (SST) was most highly correlated with the dominant common trend, and ocean productivity or circulation (measured by primary production or North Pacific Gyre Oscillation (NPGO)) with secondary trends. For most species, recent increases in SST were positively associated with body condition of all classes. In contrast, ocean productivity or circulation conditions during the past decade were more often negatively associated with mature body condition across species, while the effect of productivity on immature body condition were more variable.

## 2 Methods

Our objective was to identify common trends in fish condition across 35 species and two life-history stages of Pacific groundfishes, and to identify large-scale environmental patterns that could be causing any shared responses. The following steps are detailed in the sections below and visually summarized in Figure 1. We used morphological measurements collected from all fishery-independent surveys to maximize the sample size and seasonal representation for each species, but focus on trawl surveys for the estimation of biomass distribution (steps 1 and 4 of Figure 1) because they are the most widespread and share similar units of effort (see supplement). Because the condition of males and females at different states of reproductive development have different implications for population dynamics, observation error characteristics, and potentially even different ecological drivers, we first separated individuals and overall catches into immature, mature male and mature female classes (step 2 of Figure 1). For each sex and maturity class of each species' population, we then estimated independent spatiotemporal biomass distributions (steps 3 and 4 of Figure 1). Next, we calculated Le Cren's relative body condition deviations, modelled spatiotemporal change in these deviations, and generated a biomass density-weighted annual index of average condition for each class (steps 5, 6, and 7 of Figure 1).

To isolate possible covariation between environmental drivers and intra-specific density-dependence, we estimated the effect of local biomass density on spatiotemporal variation in body condition. When the effect of local biomass density was negative, we generated a new adjusted condition index that represents expected body condition in that year if biomass density had been constant through time. We then report two types of common trends (step 8 of Figure 1) and the strength of large scale environmental correlations with each of these trends (step 10 of Figure 1): 1) body condition across species within each of three maturity classes, and 2) body condition adjusted for local density effects across species within each of three maturity classes.

### 2.1 Splitting specimens and total catch by sex and maturity

To maximize the sample size and seasonal representation for each species, we used morphological measurements collected from all available fishery-independent multi-species surveys (see Supporting Methods A.1). Protocols for collecting individual-level data varied among surveys and species, but in most cases sub-samples of approximately 25 fish per catch event were individually weighed, measured, and sexed. Data on reproductive maturity was often only collected for most species

of commercial importance. Our analysis was therefore focused on these commercially important species; however, we used literature-based maturity thresholds for a few additional species that lacked sufficient maturity data and were of cultural or ecological interest.

We assigned individual fish to maturity classes based on the average length at 50% maturity estimated with set ID as a random effect (when maturity data was available for at least 20 sets; see Figure S3 for sample sizes and set counts):

$$M_i \sim \text{Bernoulli}(p_i), \quad (1)$$

$$p_i = \text{logit}^{-1}(\alpha + \alpha_j + \beta L_i), \quad (2)$$

$$\alpha_t \sim \text{Normal}(0, \sigma_\alpha^2), \quad (3)$$

where  $M_i$  represents the mature (1) or immature (0) status of fish  $i$ ,  $p_i$  represents the probability of maturity of fish  $i$ ,  $\alpha$  represents a global intercept,  $\alpha_j$  represents a set-level deviation for catch event  $j$  that is allowed to vary with a variance of  $\sigma_\alpha^2$ ,  $\beta$  represents a coefficient, and  $L_i$  represents the length of fish  $i$ .

For the purpose of calculating weight ratios by sex and maturity class (not for condition calculations), when lengths were known but individual weights were missing, individuals were assigned estimated weights based on the average length-weight relationship for each species:

$$\log(W_i) \sim \text{Student-t}(3, \log(a) + b \log(L_i), \sigma), \quad (4)$$

where  $W_i$  and  $L_i$  represent the weight and length for fish  $i$ ,  $a$  and  $b$  are the species-specific parameter estimates of the length-weight relationship  $W_i = aL_i^b$ ,  $\sigma$  is the observation error scale, and 3 is degrees of freedom, fixed at a low value to allow for extreme outliers among the residuals.

For each sampled tow, we then split the total catch of each species into immature, mature males, and mature females using the observed proportions by weight among the individually measured specimens. For unsampled tows, i.e., without individual-level measurements, an average from either: i) other tows within each survey-year combination; or ii) from other years or surveys was applied depending on a series of decision rules (see ‘Supporting methods A.3: Decision rules for splitting total catches from unsampled tows’).

## 2.2 Spatiotemporal estimates of biomass density

To account for possible density-dependence in body condition and to calculate a weighted average body condition, we needed spatiotemporal estimates of biomass density for each portion of each species’ population. For this purpose, we used only trawl surveys because they were the most widespread and shared similar units of effort. This meant that species exclusively associated with non-trawlable habitat could not be included in our analyses and that densities of the included species more associated with rocky substrates (e.g., inshore rockfish), may be less accurate than for other species.

First, we fit separate spatiotemporal models for the total biomass of each species using catches from all trawl surveys that had positive catches of the species in at least three years, and at least 1% positive catches overall between 2000 and 2023 (Table S2; step 1 of Figure 1). Next, we fit similar models to the estimated split catches representing relative biomass of immatures, mature males, and mature females (step 3 of Figure 1). For each maturity class, we fit two versions, which differed in the amount of data and assumptions they relied on: 1) an ‘all catches’ model that relied on average maturity ratios from other surveys or years to enable inclusion of the same tows included in the model for total biomass; and 2) a ‘sampled catches’ model including only tows from surveys in years when sufficient morphological data was collected (see ‘Supporting methods A.3: Decision rules for splitting total catches from unsampled tows’).

Because catch weights included both zeros and positive continuous values with occasional extreme values, we used a delta (hurdle) model approach (Aitchison 1955). Our two-part models used a binomial distribution for presence–absence (technically, encounter–non-encounter) and a lognormal distribution for the positive catches.

We modelled survey catch weights as representative of relative biomass density  $D$  for point in space  $s$  and time  $t$  as a product of two components,

$$D_{s,t} \sim \text{Bernoulli}(\mu_{1,s,t}) \cdot \text{Lognormal}\left(\log \mu_{2,s,t} - \frac{\vartheta^2}{2}, \vartheta^2\right), \quad (5)$$

where  $\mu_{1,s,t}$  represents the expected probability of encountering the species in a given tow,  $\mu_{2,s,t}$  represents the expected catch weight conditional on encounter, and  $\vartheta$  is the standard deviation of positive observations in log-space. These two components were modelled as a function of a series of fixed and random effects in two linear predictors where subscripts 1 and 2 denote the equivalent parameters

from the first (encounter probability) and second (positive catch) linear predictors respectively:

$$\mu_{1,s,t} = \text{logit}^{-1} (\alpha_1 + \mathbf{X}_{1,s,t}\boldsymbol{\beta}_1 + \omega_{1,s} + \epsilon_{1,s,t}), \quad (6)$$

$$\mu_{2,s,t} = \exp (\alpha_2 + \mathbf{X}_{2,s,t}\boldsymbol{\beta}_2 + \omega_{2,s} + \epsilon_{2,s,t} + O_{s,t}), \quad (7)$$

where  $\alpha$  represents the intercept for synoptic trawl surveys (see Supporting Methods A.1.1),  $\mathbf{X}_{s,t}$  represents a vector of predictors (other survey types, and second order polynomials of centered log depth in Figure S6 and date relative to the summer solstice in Figure S7),  $\boldsymbol{\beta}$  represents a vector of corresponding parameters, and  $O_{s,t}$  represents an ‘offset’ for log area swept (see ‘Supporting Methods A.2: Effort calculation for trawl surveys’).

We constrained the spatial and spatiotemporal covariance via a Matérn covariance function with the range (distance at which correlation is effectively independent) being allowed to differ between the spatial and spatiotemporal fields. The vector of  $\omega_s$  ( $\boldsymbol{\omega}$ ) represents a spatially correlated random effect (a Gaussian Markov random field; GMRF) that is constant through time and has an inverse precision (i.e., covariance) matrix  $\boldsymbol{\Sigma}_\omega$ , i.e.,  $\boldsymbol{\omega} \sim \text{MVNormal}(0, \boldsymbol{\Sigma}_\omega)$ . Each  $\epsilon_{s,t}$  term represents a value in space and time from spatiotemporally correlated random effects. The vector of spatiotemporal effects for a given year ( $\boldsymbol{\epsilon}_t$ ) were assumed to follow a spatiotemporal random walk with yearly deviations (innovations)  $\boldsymbol{\delta}_t$  that follow a GMRF:

$$\boldsymbol{\delta}_t \sim \text{MVNormal}(0, \boldsymbol{\Sigma}_\epsilon), \quad (8)$$

$$\boldsymbol{\epsilon}_{t=1} = \boldsymbol{\delta}_{t=1}, \quad (9)$$

$$\boldsymbol{\epsilon}_{t>1} = \boldsymbol{\epsilon}_{t-1} + \boldsymbol{\delta}_t. \quad (10)$$

If a species, or more often one maturity class, was too infrequently caught to support the above delta model (indicated by failure of the delta model to converge), we instead used a Tweedie distribution with a log link to accommodate zeros and positive continuous values with a single linear predictor (Tweedie 1984, Dunn and Smyth 2005, Anderson *et al.* 2019):

$$D_{s,t} \sim \text{Tweedie}(\mu_{s,t}, p, \phi), \quad 1 < p < 2, \quad (11)$$

$$\mu_{s,t} = \exp (\alpha + \mathbf{X}_{s,t}\boldsymbol{\beta} + \omega_s + \epsilon_{s,t} + O_{s,t}), \quad (12)$$

where  $\mu_{s,t}$  represents the expected biomass density,  $p$  represents the Tweedie power parameter, and

$\phi$  represents the Tweedie dispersion parameter.

We fit all spatiotemporal models with the R package sdmTMB (version 0.6.0.9004; [Anderson et al. 2024](#)), which combines automatic differentiation and the Laplace approximation from the TMB package (Template Model Builder; [Kristensen et al. 2016](#)) with the SPDE (Stochastic Partial Differential Equation) approximation to Gaussian random fields ([Lindgren et al. 2011](#)) using input finite element mesh matrices from fmesher (version 0.1.7; [Lindgren 2024](#)). We constructed the meshes with vertices at least 20 km apart. We aided estimation of marginal GMRF standard deviations,  $\sigma$ , and range parameters,  $\rho$ , (distance at which spatial correlation has decayed to  $\approx 0.13$  [Lindgren et al. 2011](#)) for all spatial and spatiotemporal fields using bivariate penalized complexity priors ([Fuglstad et al. 2019](#)), such that  $P(\sigma < 2 = 0.95)$  and  $P(\rho > \text{minimum distance between mesh vertices} = 0.95)$ . For each species, we attempted to fit the model described in Equation 5. If this resulted in unrealistic spatial parameters or was not consistent with convergence, we attempted a series of model simplifications including trying Equation 11 if even simplified versions of the delta model did not converge (see ‘Supporting Methods A.4: Model convergence and decision rules for simplifying spatiotemporal models’).

From our fitted models, we calculated area-weighted annual indices of biomass by predicting on a  $2 \times 2$  km grid covering the combined domains of the synoptic trawl surveys, summing the predicted biomass each year ([Thorson et al. 2015a](#)), and applying a generic bias-adjustment given the non-linear transformation of the random effects ([Thorson and Kristensen 2016](#)). These indices represent expected total biomass if the entire synoptic survey domain was sampled on the summer solstice with synoptic survey methods. For each species, we summed the indices of each model version across maturity classes to see how much the use of average sex/maturity ratios to split catches was causing differences from the index of total biomass. In subsequent steps, we used predictions derived from the model version (all catches vs sampled catches) that differed the least (Figure S4). Delta-lognormal models of the form described above are known to sometimes differ in scale from a design-based estimator making this check on scale consistency particularly important ([Thorson et al. 2021](#), [Dunic et al. 2025](#)).

### 2.3 Body condition index

We calculated Le Cren’s relative condition factor ( $K_{\text{rel}}$ ) as the ratio between the observed weight ( $w$ ) of a whole individual fish and the expected weight ( $K_{\text{rel}} = w/\hat{w}$ , [Le Cren 1951](#), step 5 of Figure 1). The expected weight was given by the relationship  $\hat{w} = al^b$ , where  $l$  is the observed

length and parameters  $a$  and  $b$  were estimated by equation 4 for average species-specific length-weight relationships across years and space, but calculated separately for males and females (Froese 2006). We used Le Cren’s condition factor because it is widely used in fisheries and the parameters used to calculate expected weights are derived for each species separately resulting in values centered on 1, which facilitate comparisons across species (Gubiani *et al.* 2020, Wuenschel *et al.* 2019). An individual with a  $K_{\text{rel}} = 1$  is of average weight for its length and species. To avoid bias from extreme measurement errors, individuals whose length-weight residuals exceeded twice the scale parameter for the observation error with a Student t distribution ( $\text{df} = 3$ ) were excluded from further analyses (Figure S5; Table S3 for sample sizes). Specimens of unknown sex that were smaller than the length at 50% maturity (calculated previously for splitting of total catch; Figure S3) were assigned an expected weight that was based on the average of the parameter values for males and females, while those larger than the length at 50% maturity were excluded.

We then modelled spatiotemporal variation in relative body condition  $K_{\text{rel}}$  separately for each maturity class of each species at each point in space  $s$  and time  $t$  assuming lognormal observation error

$$K_{\text{rel}} \sim \text{Lognormal} \left( \log \mu_{3,s,t} - \frac{\vartheta^2}{2}, \vartheta \right), \quad (13)$$

$$\mu_{3,s,t} = \exp \left( \alpha_3 + X_{3,s,t} \beta + \omega_{3,s} + \epsilon_{3,s,t} \right), \quad (14)$$

where  $\vartheta$  is the standard deviation in log-space,  $\alpha_3$  represents the intercept for the gear type that caught the most sampled specimens,  $X_{3,s,t}$  represents a vector of predictors (other gear types, and second order polynomial for date relative to the summer solstice in Figures S11 to S13), and  $\beta$  represents a vector of corresponding parameters (step 6 of Figure 1). We simplified the polynomial for date relative to solstice to a linear relationship when the range of sampling dates was  $< 60$ . This time we also allow for anisotropic correlation in the spatial fields, for increased flexibility since we were not interested in accounting for depth as a fixed effect (Fuglstad *et al.* 2015, Thorson *et al.* 2015a).

Next, we tested for an effect of density-dependence by adding a predictor of estimated log biomass density (total mature biomass for both mature males and females, immature estimates otherwise) to  $X_{3,s,t} \beta$  of equation 14. This variable was centred on the average estimated log density for all of the specimens included in the model. If the slope of this density effect was positive, or negative by less than the SE of this parameter (Figures S8 to S10), than we reverted to the density-agnostic model

of relative body condition in equation 14. If the models did not converge, model simplification was usually limited to forcing the spatial and spatiotemporal fields to share the same range, or dropping the spatial field entirely when the spatial random field standard deviation ( $\sigma_\omega$ ) was less than 0.001 (see ‘Supporting Methods A.4: Model convergence and decision rules for simplifying spatiotemporal models’).

From the fitted density-agnostic models for all maturity classes of each species, as well as for any models showing evidence of negative density-dependence, we calculated average Le Cren’s condition indices (step 7 of Figure 1) using the same general method as for the biomass indices (step 4 of Figure 1). This time, however, we weighted the local estimates of condition by the proportion of each year’s predicted biomass that occurred in each cell rather than the area of the cell (Indivero *et al.* 2023, Lindmark *et al.* 2023). For models adjusting for density-dependence, the weighting was the same but the local predictions depended on the mean across all years of the estimated local biomass densities (generated in step 3 of Figure 1). The density-agnostic indices represent the estimated average body condition of an individual fish belonging to a species and class, while the adjusted indices represent expected average body condition if local biomass density was constant through time (although weighted by actual annual abundance distributions).

## 2.4 Identify common trends

We used Bayesian Dynamic Factor Analysis (DFA) (Ward *et al.* 2019) to identify shared trends across species in our indices of body condition (step 8 of Figure 1). This approach consists of two components: one describing the latent processes or trends (which represent shared patterns among time series); and one linking these processes to the observations. We modelled the latent trends as first-order autoregressive (AR1) processes, such that the value of the  $l$ -th latent trend  $x$  at time  $t + 1$  is represented by  $x_{l,t+1} = \phi_l x_{l,t} + n_{l,t}$ , where the trend approaches a random walk as  $\phi$  approaches 1 and the trend behaves as white noise at  $\phi = 0$ , and where deviations  $n_{l,t}$  are modelled as standard normal white noise  $n_{l,t} \sim \text{Normal}(0, 1)$ . The latent trend values  $x_{l,t}$  are linked to the observed condition index values  $y_{i,t}$  via a loadings matrix  $Z$  such that value  $Z_{i,l}$  represents an effect of trend  $l$  on time series  $i$ , which is static through time:

$$y_{i,t} = Z_{i,l}x_{l,t} + e_{i,t}, \tag{15}$$

$$e_{i,t} \sim \text{Normal}(0, \tau_i^2/w_{i,t}), \tag{16}$$

where  $e_{i,t}$  is observation error and  $\tau_i^2/w_{i,t}$  is the variance of that observation error. This variance is decomposed into an estimated scaling parameter  $\tau$  and an inverse variance weight  $w_{i,t}$  calculated as the inverse of the squared standard error of  $\widehat{K}_{\text{rel},i,t}$  for timeseries  $i$  and year  $t$ . This weighting propagates the relative precision of the condition time series from the previous models.

We fit the DFA models with the R package `bayesdfa` version 1.3.3 (Ward *et al.* 2019), which samples from the joint posterior of DFA models using the No-U Turn Sampler (NUTS) Markov chain Monte Carlo (MCMC) algorithm via `rstan` (Hoffman and Gelman 2014, Carpenter *et al.* 2017, Stan Development Team 2022). Because the elements of  $\mathbf{x}$  (trends) or  $\mathbf{Z}$  (loadings) may flip sign within an MCMC chain, or multiple chains may converge on parameters that are identical in magnitude but with different signs, `bayesdfa` applies constraints and priors on  $\mathbf{Z}$  and flips the posterior samples of MCMC chains relative to the first chain as needed to ensure that the sign of the estimated quantities is the same across chains (Ward *et al.* 2019). To aid convergence, we also standardized each condition index (by subtracting the mean and dividing by the standard deviation) prior to fitting and set the intercepts equal to zero.

We analyzed each maturity class separately because of inherent differences in the physiological and demographic implications of variation in each class. We first considered all unadjusted, density-agnostic condition indices, and then repeated each DFA with indices adjusted to exclude any apparent negative effects of local density-dependence. We attempted to identify up to four latent trends, but a maximum of two were simultaneously able to explain meaningful variation across the time series and achieve satisfactory convergence criteria. We sampled from five MCMC chains for 10,000 iterations with a target acceptance ratio (“adapt delta”) of 0.95 and a maximum tree depth of 12 in `rstan`. We discarded the first half of each chain as warm-up. We assessed convergence by visual inspection of chains and ensuring potential scale reduction, or split  $\hat{R}$ , statistics were  $< 1.01$  and bulk effective sample sizes were  $> 400$  for all parameters (Vehtari *et al.* 2021).

## 2.5 Test for environmental correlates

We selected a set of potentially relevant environmental variables from those available for Pacific Canadian waters in the `pacea` R package (Edwards *et al.* 2024). For each variable, we calculated standardized indices for January through June of each year (months leading up to the summer solstice for which we predicted our indices) and the entire preceding year (step 9 of Figure 1). We chose to focus on the Oceanic Niño Index (ONI), the Pacific Decadal Oscillation (PDO) and the North Pacific Gyre Oscillation (NPGO). ONI classifies El Niño (warm) and La Niña (cool) events in the eastern

tropical Pacific, while the latter indices are respectively the first and second principal components of sea-surface height anomalies. The ONI and PDO are the most widely used Pacific indices, while the NPGO has been associated with changes in strength of the North Pacific Current, surface salinity, and upper ocean nutrients (Di Lorenzo *et al.* 2008, 2009), and leads primary production by two years for the Canadian Pacific region (Peña *et al.* 2019).

We also considered variables from the British Columbia continental margin (BCCM) coupled physical-biogeochemical Regional Ocean Modeling System (ROMS; Peña *et al.* 2019). However, these model outputs were only available through 2019, so for sea surface temperature we used NOAA’s spatial Optimum Interpolation (OI) instead (shown in red alongside the BCCM surface and sea floor temperatures, in pink and orange respectively, on middle panel of step 9 in Figure 1). Of the BCCM variables, depth-integrated primary production was negatively related to bottom oxygen concentration, likely either through upwelling of nutrient-rich oxygen depleted waters or the subsequent decomposition of organic matter, so when testing for an effect of seafloor oxygen availability we inverted the concentration (multiplying by -1) to represent degree of depletion (bottom panel of step 9 in Figure 1). These spatially and temporally explicit variables were first projected to a  $2 \times 2$  km grid covering Canada’s Pacific Ocean Exclusive Economic Zone. From this projection, we then calculated a mean of monthly mean values for April through June (January through June for primary production to allow more time for bottom-up trophic effects) for polygon encompassing the continental shelf (illustrated by the blue area in Figure S14). Additional variables such as surface phytoplankton and surface oxygen concentrations were available, but were considered less likely to be relevant for most groundfish species than depth integrated or bottom concentrations, so we did not include them in the final variable set for this analysis.

We assessed correlations between each identified latent trend (hereafter, referred to as common trends to draw attention to their basis in shared patterns among species) and each environmental variable using post-hoc tests that propagated uncertainty in the trends (similar to Litzow *et al.* 2020, step 10 of Figure 1). Specifically, we took 1000 samples from each DFA trend posterior and calculated a correlation with a given environmental time series in a Bayesian rstan model for each of those 1000 samples. Each correlation model was fit with a single chain and 300 iterations discarding the first 150 as warm-up. We then combined all 150,000 samples into a single posterior. This integrates over the uncertainty in the DFA trend posteriors. The correlation model included a Student-t prior on the Gaussian observation error with 3 degrees of freedom and a scale parameter of 2 and a uniform prior between -1 and 1 for the correlation coefficient. We illustrate the strength of the correlations

between each trend and the two variables which showed to strongest relationships using posteriors histograms. Common trends from any model can be inverted (multiplied by -1) and end up with exactly the same model as long as the respective loadings are also flipped; therefore, we choose the trend orientation that resulted in a positive association with these variables so that species-specific loadings would represent positive or negative associations with both the trend and its correlated variables. In addition, NPGO was inverted for easier comparison with primary production, because NPGO scores tend to be negatively associated with upwelling and primary production along this coast. Variables representing the previous year's conditions were only tested against common trends for females due to the greater potential for a lagged effect on reproductive output than on energy stores.

All analyses were conducted in R version 4.4.1 (R Core Team 2024). Code used for these analyses is available at <https://github.com/pbs-assess/gfcondition> and will be archived at Zenodo on publication.

## 3 Results

### 3.1 Sex and maturity specific biomass indices

Among a suite of 35 commercially, culturally, and ecologically important groundfish species occurring in Pacific Canadian waters, many species showed an overall coastwide increase in their trawl survey vulnerable biomass indices over the last two decades (2000–2024; Figure 2). Maturity- and sex-specific biomass ratios varied between species and over time within species with patterns ranging from all maturity classes showing relatively steep declines (e.g., Pacific Spiny Dogfish, hereafter ‘dogfish’), all classes showing sharp increases (e.g., Bocaccio and Slender Sole), to asynchronous fluctuations (e.g., Lingcod; Figure 2). As expected, mature males and females of the same species showed more similar patterns to each other than to their immature counterparts. For some species, peaks in immature biomass indices preceded notable increases in mature biomass (e.g., Bocaccio, Lingcod, Slender Sole, Yellowmouth Rockfish), although for Pacific Cod and Sablefish the opposite (peaks in mature biomass preceding increases in immature biomass) appeared to occur (Figure 2). The ‘all catches’ approach with imputed ratios of maturity classes for unsampled survey catches produced indices that when summed matched overall biomass indices more closely than the ‘sampled catches’ approach for most species (with exceptions being Big Skate, English Sole, Lingcod, Pacific Ocean Perch, Sablefish, and Yelloweye Rockfish; Figure S4).

## 3.2 Body condition indices

After accounting for spatial and temporal variability in sampling, trends in average body condition over time also varied within and between species, although mature males and females of the same species generally showed more similar patterns to each other than to their immature counterparts (Figure 3). Uncertainty in condition estimates varied from relatively precise for abundant and frequently sampled species, such as Arrowtooth Flounder ( $> 60,000$  specimens measured), to too broad to draw any conclusions for more rarely encountered species, such as Shortraker Rockfish ( $\sim 2000$  specimens; Table S3). When the estimated effect of local biomass density was negative (Figures S8 to S10), the recalculated body condition indices that excluded this effect of density-dependence tended not to differ substantively in the overall trends (dashed lines in Figure 3). The only exception was mature female Longnose Skate, for which the condition index appeared more variable when accounting for density. However, common trends identified from DFAs using condition indices that excluded any negative effects of density-dependence (Figures 4 to 6 black line and shading in top row) tended to have slightly tighter confidence intervals and more distinct fluctuations than those without adjusting for density dependence (Figures S15 to S17 black line and shading in top row). Despite this, the general patterns identified were nearly identical with or without adjusting for density-dependence. The common trends identified for all immatures and mature females showed stronger loadings for more species than for mature males (indicated by more of the darkest violins in Figures 4 and 6 than in Figure 5). For most species, changes in body condition were better explained by one or the other of the two identified common trends; however, across all species, the strongest loadings belonged to trend 1.

## 3.3 Environmental correlates of body condition

For all sex and maturity classes, common trends in body condition were correlated with SST (trend 1) and with NPGO (trend 2), where the correlation with NPGO was strongest with a 2-year lag (as indicated by histograms of post-hoc correlation coefficients in Figure 4 middle row). For immatures, PDO (trend 1) and primary production (based on a shorter time series than the other correlations; trend 2) were also fairly strongly correlated with each common trend. For mature males, common trends in body condition were most associated with all the same environmental variables as immatures, but correlations were less strong (Figure 5 middle row). For mature females, trend 1 was still most associated with SST, while both NPGO on a 2-year lag and PDO were associated with

trend 2 (Figure 6 middle row). Current year primary production was not correlated with either female trend, but the previous year's production was weakly correlated with trend 1 (Figure 6 left column).

Once common trends are oriented in a direction for which the dominant environmental associations are positive for all maturity classes, the signs of species-specific loadings are suggestive of their environmental responses. Because primary production and NPGO are related and appeared to have opposing effects, we inverted NPGO (Figures 4 to 6). PDO was positively correlated the chosen orientations of trend 1 but negatively with trend 2, so we inverted PDO when compared with trend 2 (Figure 6).

The species and maturity classes whose average body condition were most likely to be negatively associated with average coaswide SST (or possibly PDO in the case of immatures), based on strong negative loadings on trend 1, were immature Bocaccio and Yellowtail Rockfish, immature and mature male Walleye Pollock, mature male and female Southern Rock Sole, and mature female Yelloweye, Quillback, and Redbanded Rockfish (left column of loadings in Figures 4 to 6). Meanwhile, species most positively associated with these same trends were Arrowtooth Flounder and Rex and Dover Sole (all sex and maturity classes), both sexes of mature Petrale Sole, Greenstriped Rockfish, Lingcod and dogfish, immature and mature male Sablefish, immature Redbanded Rockfish, mature male Canary Rockfish, and mature females of several additional species.

Primary production and inverted lagged-NPGO were both strongly positively correlated with our selected immature trend 2 orientation (Figure 4). As such, immature condition of Spotted Ratfish, English and Southern Rock Sole, Quillback and Greenstriped Rockfish, dogfish, and Longnose Skate all appeared likely to be correlated positively with primary production or negatively with NPGO. In contrast, condition of immature Pacific Cod, Lingcod, Sablefish, Pacific Ocean Perch, and several rockfish species were negatively loaded on this trend and, therefore, with these variables. Trend 2 was “wigglier” (less linear) for mature fish than for immatures, and for females than for males (top right in Figures 4 to 6). For mature males, trend 2 was less strongly correlated with any of the environmental covariates tested, but primary production and inverted lagged-NPGO still had the strongest correlations (Figure 5). For mature females, trend 2 was still strongly correlated with inverted NPGO, and due to the increased wiggleness also, though more weakly, with inverted PDO. Similar to the pattern seen for immatures, mature Spotted Ratfish and some of the flatfish (e.g., Dover and Slender Sole) had positive loadings, while most rockfish species had negative loadings on this trend.

## 4 Discussion

We generated indices of body condition, and identified common trends among them, for 35 species belonging to a commercially, culturally, and ecologically important demersal fish assemblage in the Canadian waters of the Pacific Ocean. Each index was spatiotemporally standardized and sex and maturity-specific. Common trends among immature fish and mature females explained more of the variation in body condition for more species (higher loadings) and were more tightly correlated with the environmental variables we investigated, than they were for mature males. Across species for all sex and maturity classes, the dominant common trend (trend 1) was most highly correlated with sea surface temperature (SST), and the secondary trend (trend 2) with some aspect of ocean upwelling or productivity (i.e., NPGO on a two-year lag). Body condition of most species, regardless of sex or maturity, seemed either neutrally or positively correlated with warmer SST. Exceptions that showed declining body condition at higher temperatures were immature Bocaccio and Yellowtail Rockfish, both immature and mature male Walleye Pollock, both sexes of mature Southern Rock Sole, and mature female Yelloweye, Quillback, and Redbanded rockfishes. Only immature body condition appeared strongly correlated with both primary production and inverted NPGO two springs prior, but among species this effect was equally likely to be negative (e.g., dogfish, Lingcod, Sablefish) as positive (e.g., Quillback Rockfish, Southern Rock Sole, Spotted Ratfish). Mature body condition was much more strongly influenced by NPGO, such that flatfish (e.g., Dover and Slender Sole) tended to be heavier for a given length when the index was negative two springs prior, while most rockfish species were heavier when it was positive two springs prior. NPGO is related to nutrient availability and productivity with a 2-year lag for the Canadian Pacific coast (Peña *et al.* 2019).

Our approach of generating spatiotemporally standardized, sex and maturity-specific indices of body condition and investigating common trends across species reduces the need for understanding precise species-specific relationships, while increasing the potential to detect community-level drivers of productivity. However, when a shared trend is strongly correlated with a particular environmental variable, each species' index loading on that trend can be interpreted as indicating how negatively or positively its condition is impacted by that variable. Species-specific local environmental effects on body condition have previously been investigated using spatiotemporal models, although the explanatory power of local covariates on individual condition has generally been found to be far lower than that of spatial and spatiotemporal latent variables, suggesting missing variables and/or mismatches in spatial or temporal resolution (Thorson 2015, Lindmark *et al.* 2023). In such studies,

temperature has often been found to be associated with changes in body condition (Thorson 2015, Grüss *et al.* 2020, Lindmark *et al.* 2023, Somov *et al.* 2024), although its effect may vary with latitude. Of the 20 species we investigated that were also included in Thorson (2015), Arrowtooth Flounder, Yellowtail and Canary Rockfish, Shortspine Thornyhead, and Sablefish were found to be negatively impacted by increasing temperature in California Current waters to the south. Of these species, only immature Yellowtail also appeared negatively associated with temperature in Canadian waters; while, in contrast, Arrowtooth Flounder and Sablefish of all classes, and mature Canary Rockfish seemed to benefit from warmer conditions. All other species were either consistently in better condition when temperatures were warmer or seemingly not impacted. Further north, in the Bering Sea, Grüss *et al.* (2020) found that the coldest and warmest years were associated with low and high abundance-weighted condition, respectively, for Arrowtooth Flounder, Flathead Sole, Pacific Cod, and Walleye Pollock, although this pattern may have been confounded by changes in abundance due to weighting by total abundance rather than proportional abundance.

The effects of temperature on growth have been shown to vary with factors such as age, sex, size, latitude and local environmental conditions (Lloret 2002, Brosset *et al.* 2017, Lindmark *et al.* 2022). Therefore, our finding of variability among species, sex and life stage was not unexpected. Temperature can affect growth and condition of marine fishes through direct physiological impacts on consumption and metabolism (Lindmark *et al.* 2022, Robinson *et al.* 2024) and/or through exogenous factors such as availability of prey, prevalence of disease or local habitat quality (Lloret 2002, Casini *et al.* 2006, Boldt and Rooper 2009, Champion *et al.* 2020). For example, Lloret (2002) reported differences in condition among adult males, adult females and juveniles for 10 demersal species in the Mediterranean Sea, with adults generally being in better condition than juveniles and, among adults, females better than males. They did not directly evaluate the effects of temperature but reported that fish in shallower habitats were generally in better condition. Likewise, Rätz and Lloret (2003) found that Atlantic cod stocks occurring in colder, more northern waters were in poorer condition than stocks in warmer waters, which they attributed to better food supply and physiological conditions in warmer waters. However, several studies of forage fish species have found the opposite. The 2016 marine heatwave in the north Pacific Ocean appeared to have direct physiological effects on Pacific sand lance, lowering their winter body condition, resulting in growth failure of the 2015 year class, and negative impacts on seabird predators in 2016 (Robinson *et al.* 2024). Anchovy and sardine in the Mediterranean Sea also showed regional variation but a general downward trend in condition during a period associated with warming temperatures (1975–2015); however,

the authors concluded that the overall decrease was most likely caused by regional environmental effects including mezoplankton concentrations (Brosset *et al.* 2015, 2017). While we did not find a strong correlation between average bottom oxygen concentrations and our common trends, primary production and NPGO can impact oxygen bottom availability through processes such as upwelling and decomposition. Indeed, more species were negatively associated with the trend associated with primary production than positively associated, suggesting that excess primary production can have negative impacts on condition (potentially through hypoxia). Among these were immature Sablefish, Dogfish, and Lingcod, and most mature rockfish. These contrasting effects, which may also be mediated by density-dependent effects (Casini *et al.* 2006, 2016b, Grüss *et al.* 2020, Rindorf *et al.* 2022), highlight that impacts of temperature and other environmental variables on body condition are highly regionally and species-specific.

While population density and condition often respond similarly to local environmental conditions or prey abundance resulting in a positive correlation between them, increases in local density can also result in increased competition for food and potentially a decrease in condition (Thorson 2015, Grüss *et al.* 2020). Therefore, detection of density-dependence depends on selection of appropriate spatial scales and covariates (Ray and Hastings 1996, Michalsen 1998, Thorson *et al.* 2015b). By accounting for spatial and spatiotemporal variability in condition using spatial random fields, as well as estimating the effect of changes in local density over time, we were able to identify negative intra-specific density dependence in 12 of 35 species for immatures, and likewise for mature males and/or females (but only four species showed it for both immatures and a mature class). Thorson (2015) and Lindmark *et al.* (2023) treated intra-specific density as a covariate in a similar way to the present study, although density and condition can also be modelled simultaneously (Grüss *et al.* 2020, Somov *et al.* 2024). For the California Current species also included in our analysis, Thorson (2015) found negative effects of density for two out of five flatfishes (Petrale Sole and Arrowtooth Flounder) and two out of 12 rockfishes (Bocaccio and Shortspine Thornyhead). Of these, negative density-dependence was not found for any mature flatfish in Canadian waters, but was for immature Arrowtooth Flounder, English Sole, and Pacific Sanddab. For rockfishes, we found negative density-dependence in seven of these California Current species, with more cases among the mature classes than immature (i.e., in immature Greenstriped, Shortspine Thornyheads, in mature Darkblotched, Pacific Ocean Perch, and Widow of both sexes, and in mature female Yelloweye and Yellowtail). Grüss *et al.* (2020) found also found negative spatial and spatiotemporal correlations between density and body condition for Arrowtooth Flounder in the Bering Sea after accounting for effects of local

bottom temperature. We found that adjusting for these local-scale effects of density-dependence did not have a strong impact on species-specific or common trends in body condition; however, there are many other dimensions, such as spatial, temporal and inter-specific effects that could be explored. For example, evidence for an inter-specific competitive effect on Atlantic Cod body condition was slightly stronger at a scale of approximately  $2500 \text{ km}^2$  (ICES rectangles; [Lindmark et al. 2023](#)) than at the scales estimated in the present study.

Body condition is also highly seasonal, determined by annual cycles of food availability, growth and gonad development ([Le Cren 1951](#), [Dutil et al. 1995](#), [Brosset et al. 2015](#)). The weights using in our condition calculation were from whole fish, gonads included, so seasonal effects are confounded with variation in reproductive investment, though likely more so for mature females than for males and immature fish ([Le Cren 1951](#)). We attempted to minimize seasonal effects in our analyses by controlling for date in generating the indices and considering sex and maturity classes separately. For this reason, and because our observations were collected from surveys that are conducted only during the summer period, our indices represent a single snapshot of condition each year. It is possible that condition measurements taken at different times of the year could better inform our understanding of population productivity and the factors influencing condition ([Dutil et al. 1995](#)). However, other studies of environmental correlates with condition have also focused on indices calculated with data from one season ([Brosset et al. 2015](#), [Casini et al. 2016b](#), [Grüss et al. 2020](#)). For example, [Casini et al. \(2016b\)](#) calculated condition indices from an Autumn survey, as this represented the main feeding season for cod in their study. While surveys in Canadian Pacific waters are almost exclusively conducted in the summer, commercial biological samples are frequently collected year-round. Unfortunately, this sampling often relies on lengths alone to assess fish size, and does not include the weighing of individual specimens. However, if the appropriate measurements are collected, the potential exists to expand the seasonal scope of studies like this. However, controlling for spatial and size selectivity will be especially important due to the potential for biases caused by selective sampling. We suggest this could be a fruitful avenue of future research into the seasonal influence of environmental factors on condition and productivity for individual species.

Other areas for further research and improvement include propagation of uncertainty, alternative ways of measuring body condition, and the inclusion of alternative drivers and confounding factors in DFA correlations. We propagated uncertainty at several steps (condition to DFA and from DFA to posthoc correlations), but the condition and density models could be estimated simultaneously (e.g., [Grüss et al. 2020](#)). One limitation of Le Cren's relative condition, common to several other

condition indices, is that it is correlated with body size, potentially causing bias in the residuals used to calculate the index (Peig and Green 2009, 2010). Other indices could be applied within our framework (e.g., the scaled mass index of Peig and Green (2009)) that might be more effective at isolating body condition changes from growth than our strategy of splitting into sex- and maturity-specific groups (Peig and Green 2010). As described in the methods, we tested only a small suite of potential environmental variables and only considered lags for females in response to primary production (due to confounding effects of reproductive output) or when otherwise specifically justified in the literature. However, this still amounts to many more tests than we include in the results where only the two strongest correlations detected for each trend have been discussed. Finally, the alternative drivers and confounding factors such as population or guild-level density dependence could be included within the DFA. Doing so would require relatively long time series but could be contrasted with standardizing for these covariates when forming the condition index, as we did here for density dependence.

Numerous studies have advocated including fish body condition in stock assessment advice (Dutil *et al.* 1995, Rätz and Lloret 2003, Casini *et al.* 2016a, Van Deurs *et al.* 2023, Boldt *et al.* 2025). Body condition is linked with the two productivity components of modern stock assessments that are most difficult to predict: recruitment and survival (or natural mortality). Fish in poor condition are more likely to experience increased natural mortality due to mechanisms such as starvation, disease, and vulnerability to fishing gear (Dutil *et al.* 1995, Casini *et al.* 2016a, Dutil and Lambert 2000, Regular *et al.* 2022). Rätz and Lloret (2003) reported a positive relationship between body condition and the alpha parameter of the Ricker (1954) stock-recruit model, indicating that stocks in better condition had a better chance of good recruitment at low stock size, and the corollary, that stocks in poor condition will have less robust recruitment at low stock size. Van Deurs *et al.* (2023) found that average weight-at-age of old spawners was a better predictor of recruitment than either the proportion of old spawners or the average age of spawners in 11 North Sea fish stocks. Other studies have similarly demonstrated a positive predictive relationship between condition and recruitment (Marshall and Frank 1999, Marshall *et al.* 1999, Friedland *et al.* 2015, Heintz *et al.* 2013, Brosset *et al.* 2020). Given the tendency of environment-recruitment relationships to break down over time (Myers *et al.* 1995, Myers 1998, Tamburello *et al.* 2019), condition indices, which are relatively straightforward to calculate, may provide early warning signals of recruitment or mortality events in the near term (Lambert and Dutil 1997, Brosset *et al.* 2020, Regular *et al.* 2022, Van Deurs *et al.* 2023) and would be straightforward additions to stock assessment reports (DFO 2023, Boldt

*et al.* 2025, DFO 2025). Boldt *et al.* (2025) have suggested including body condition information and other environmental variables in fishery risk assessments or report cards (Dorn and Zador 2020) to better incorporate ecosystem information into management advice.

As marine ecosystems respond to rapidly changing global climate conditions, fish body condition is likely to be an important tool for improving marine ecosystem forecasts and other approaches to designing climate-resilient fisheries management (Bolin *et al.* 2021, Mason *et al.* 2023, Carruthers 2024). Our approach propagates uncertainty from body condition estimation through to environmental correlations and has the benefit of both providing an ecosystem perspective of shared responses across an assemblage of species while also providing species-specific inference. Ultimately, robust estimates of relationships between condition, and hence energy reserves, and environmental variables could inform a risk-equivalent approach to fisheries management (e.g., Dorn and Zador 2020, Duplisea *et al.* 2021, Roux *et al.* 2022) by enabling short-term forecasts of weight-at-age, recruitment, or productivity under alternative climate regimes.

## 5 Acknowledgements

This work was supported by the Fisheries and Oceans Canada’s Competitive Science Research Fund (CSRF). It also would not have been possible without the many individuals who have contributed to collecting the survey data on which this manuscript is based. We particularly wish to thank the Groundfish surveys teams (M.R. Wyeth, N. Olsen, K. Castle, S. Hardy, K. Temple) and ship and Coast Guard crews. We also thank M.R. Siegle for comments that improved this manuscript.

## 6 Data availability statement

Most data are available at [open.canada.ca](https://open.canada.ca); however, the specific data used in this analysis, including all minor surveys and specimen records, will be archived with the code on Zenodo at the time of publication. All code used in data wrangling, analyses, and visualization is also available in a public GitHub repository: <https://github.com/pbs-assess/gfcondition>.

## 7 Conflict of Interest

The authors declare no conflicts of interest.

## 8 Bibliography

- Aitchison, J. (1955) On the distribution of a positive random variable having a discrete probability mass at the origin. *Journal of the American Statistical Association* **50**, 901. doi:10.2307/2281175.
- Anderson, S., Keppel, E.A. and Edwards, A.M. (2019) A reproducible data synopsis for over 100 species of British Columbia groundfish. *DFO Can. Sci. Advis. Sec. Res. Doc.* **2019/041**, vii + 321 p.
- Anderson, S.C., Ward, E.J., English, P.A., Barnett, L.A.K. and Thorson, J. (2024) sdmTMB: An R package for fast, flexible, and user-friendly generalized linear mixed effects models with spatial and spatiotemporal random fields. *In press at Journal of Statistical Software.* bioRxiv **2022.03.24.485545**. doi:10.1101/2022.03.24.485545.
- Boldt, J.L. and Rooper, C.N. (2009) Abundance, condition, and diet of juvenile Pacific ocean perch (*Sebastes alutus*) in the Aleutian Islands. *Fishery Bulletin* **107**, 278–285.
- Boldt, J.L., Rooper, C.N., Cleary, J., Fu, C. *et al.* (2025) Incorporating ecosystem information into science advice for fisheries management – a case study for Haida Gwaii Pacific Herring. *Canadian Journal of Fisheries and Aquatic Sciences* **82**, 1–26. doi:10.1139/cjfas-2024-0150.
- Bolin, J.A., Schoeman, D.S., Evans, K.J., Cummins, S.F. and Scales, K.L. (2021) Achieving sustainable and climate-resilient fisheries requires marine ecosystem forecasts to include fish condition. *Fish and Fisheries* **22**, 1067–1084. doi:10.1111/faf.12569.
- Boudreau, S.A., Anderson, S.C. and Worm, B. (2015) Top-down and bottom-up forces interact at thermal range extremes on American lobster. *Journal of Animal Ecology* **84**, 840–850. doi:10.1111/1365-2656.12322.
- Brander, K.M. (2007) Global fish production and climate change. *Proceedings of the National Academy of Sciences* **104**, 19709–19714. doi:10.1073/pnas.0702059104.
- Brosset, P., Ménard, F., Fromentin, J., Bonhommeau, S. *et al.* (2015) Influence of environmental variability and age on the body condition of small pelagic fish in the Gulf of Lions. *Marine Ecology Progress Series* **529**, 219–231. doi:10.3354/meps11275.
- Brosset, P., Fromentin, J.M., Van Beveren, E., Lloret, J. *et al.* (2017) Spatio-temporal patterns and environmental controls of small pelagic fish body condition from contrasted Mediterranean areas. *Progress in Oceanography* **151**, 149–162. doi:10.1016/j.pocean.2016.12.002.
- Brosset, P., Smith, A.D., Plourde, S., Castonguay, M., Lehoux, C. and Van Beveren, E. (2020) A fine-scale multi-step approach to understand fish recruitment variability. *Scientific Reports* **10**, 16064. doi:10.1038/s41598-020-73025-z.
- Bryndum-Buchholz, A., Boyce, D., Tittensor, D., Christensen, V., Bianchi, D. and Lotze, H. (2020) Climate-change impacts and fisheries management challenges in the North Atlantic Ocean. *Marine Ecology Progress Series* **648**, 1–17. doi:10.3354/meps13438.
- Carpenter, B., Gelman, A., Hoffman, M.D., Lee, D. *et al.* (2017) Stan: A Probabilistic Programming Language. *Journal of Statistical Software* **76**. doi:10.18637/jss.v076.i01.
- Carruthers, T.R. (2024) Developing the climate test: performance metrics of climate robustness. *International Commission for the Conservation of Atlantic Tunas Collective Volume of Scientific Papers* **81**.

- Casini, M., Cardinale, M. and Hjelm, J. (2006) Inter-annual variation in herring, *Clupea harengus*, and sprat, *Sprattus sprattus*, condition in the central Baltic Sea: What gives the tune? *Oikos* **112**, 638–650. doi:10.1111/j.0030-1299.2006.13860.x.
- Casini, M., Eero, M., Carlshamre, S. and Lövgren, J. (2016a) Using alternative biological information in stock assessment: Condition-corrected natural mortality of Eastern Baltic cod. *ICES Journal of Marine Science: Journal du Conseil* **73**, 2625–2631. doi:10.1093/icesjms/fsw117.
- Casini, M., Käll, F., Hansson, M., Plikshs, M. *et al.* (2016b) Hypoxic areas, density-dependence and food limitation drive the body condition of a heavily exploited marine fish predator. *Royal Society Open Science* **3**, 160416. doi:10.1098/rsos.160416.
- Champion, C., Hobday, A.J., Pecl, G.T. and Tracey, S.R. (2020) Oceanographic habitat suitability is positively correlated with the body condition of a coastal-pelagic fish. *Fisheries Oceanography* **29**, 100–110. doi:10.1111/fog.12457.
- Choromanksi, E.M., Workman, G. and Fargo, J. (2005) Hecate Strait multispecies bottom trawl survey, GGS W.E. Ricker, May 19 to June 7, 2003. *Can. Data Rep. Fish. Aquat. Sci.* **1169**, viii + 85 p.
- de Blois, S. (2020) The 2019 Joint U.S.–Canada Integrated Ecosystem and Pacific Hake Acoustic-Trawl Survey: Cruise Report SH-19-06. *U.S. Department of Commerce, NOAA Processed Report NMFS-NWFSC-PR-2020-03*. URL <https://doi.org/10.25923/p55a-1a22>.
- DFO (2023) Arrowtooth Flounder (*atheresthes stomias*) stock assessment for British Columbia in 2021. *DFO Can. Sci. Advis. Sec. Sci. Advis. Rep.* **2023/042**.
- DFO (2025) Assessment of Petrale Sole in British Columbia in 2024. *DFO Can. Sci. Advis. Sec. Sci. Advis. Rep.* **2025/002**. URL [https://www.dfo-mpo.gc.ca/csas-sccs/Publications/SAR-AS/2025/2025\\_002-eng.html](https://www.dfo-mpo.gc.ca/csas-sccs/Publications/SAR-AS/2025/2025_002-eng.html).
- Di Lorenzo, E., Fiechter, J., Schneider, N., Bracco, A. *et al.* (2009) Nutrient and salinity decadal variations in the central and eastern North Pacific. *Geophysical Research Letters* **36**. doi:10.1029/2009GL038261.
- Di Lorenzo, E., Schneider, N., Cobb, K.M., Franks, P.J.S. *et al.* (2008) North Pacific Gyre Oscillation links ocean climate and ecosystem change. *Geophysical Research Letters* **35**. doi:10.1029/2007GL032838.
- Doherty, B., Benson, A.J. and P., C.S. (2019) Data summary and review of the PHMA hard bottom longline survey in British Columbia after the first 10 years (2006-2016). *DFO Can. Tech. Rep. Fish. Aquat. Sci.* **2019/3276**, ix + 75 p.
- Dorn, M.W. and Zador, S.G. (2020) A risk table to address concerns external to stock assessments when developing fisheries harvest recommendations. *Ecosystem Health and Sustainability* **6**, 1813634. doi:10.1080/20964129.2020.1813634.
- Dulvy, N.K., Rogers, S.I., Jennings, S., Stelzenmüller, V., Dye, S.R. and Skjoldal, H.R. (2008) Climate change and deepening of the North Sea fish assemblage: A biotic indicator of warming seas. *Journal of Applied Ecology* **45**, 1029–1039. doi:10.1111/j.1365-2664.2008.01488.x.
- Dunic, J. and Anderson, S. (2025) Assessing the quality of groundfish population indices derived from the Small-mesh Multi-species Bottom Trawl Survey. Technical Report Can. Tech. Rep. Fish. Aquat. Sci. nnn.

- Dunic, J.C., Conner, J., Anderson, S.C. and Thorson, J.T. (2025) The generalized gamma is a flexible distribution that outperforms alternatives when modelling catch rate data. *ICES Journal of Marine Science* **82**, fsaf040. doi:10.1093/icesjms/fsaf040.
- Dunn, P.K. and Smyth, G.K. (2005) Series evaluation of Tweedie exponential dispersion model densities. *Statistics and Computing* **15**, 267–280. doi:10.1007/s11222-005-4070-y.
- Duplisea, D.E., Roux, M.J., Hunter, K.L. and Rice, J. (2021) Fish harvesting advice under climate change: A risk-equivalent empirical approach. *PLOS ONE* **16**, e0239503. doi:10.1371/journal.pone.0239503.
- Dutil, J.D., Chouinard, G.A. and Fréchet, A. (1995) Fish condition: What should we measure in cod (*Gadus morhua*)? Technical Report DFO Atlantic Fisheries Research Document 95/11.
- Dutil, J.D. and Lambert, Y. (2000) Natural mortality from poor condition in Atlantic cod (*Gadus morhua*). *Canadian Journal of Fisheries and Aquatic Sciences* **57**, 826–836. doi:10.1139/f00-023.
- Edwards, A., Tai, T., Watson, J., Peña, M. *et al.* (2024) pacea: An R package of Pacific ecosystem information to help facilitate an ecosystem approach to fisheries management. URL <https://github.com/pbs-assess/pacea>.
- English, P.A., Ward, E.J., Rooper, C.N., Forrest, R.E. *et al.* (2021) Contrasting climate velocity impacts in warm and cool locations show that effects of marine warming are worse in already warmer temperate waters. *Fish and Fisheries* **23**, 239–255. doi:10.1111/faf.12613.
- Evans, R., English, P.A., Gauthier, S. and Robinson, C.L. (2023) Quantifying the effects of extreme events and oceanographic variability on the spatiotemporal biomass and distribution of two key euphausiid prey species. *Frontiers in Marine Science* **10**, 1031485. doi:10.3389/fmars.2023.1031485.
- Francis, R. and Shotton, R. (1997) “Risk” in fisheries management: A review. *Canadian Journal of Fisheries and Aquatic Sciences* **54**, 1699–1715. doi:10.1139/f97-100.
- Free, C.M., Thorson, J.T., Pinsky, M.L., Oken, K.L., Wiedenmann, J. and Jensen, O.P. (2019) Impacts of historical warming on marine fisheries production. *Science* **363**, 979–983. doi:10.1126/science.aau1758.
- Friedland, K.D., Leaf, R.T., Kristiansen, T. and Large, S.I. (2015) Layered effects of parental condition and larval survival on the recruitment of neighboring haddock stocks. *Canadian Journal of Fisheries and Aquatic Sciences* **72**, 1672–1681. doi:10.1139/cjfas-2015-0084.
- Froese, R. (2006) Cube law, condition factor and weight-length relationships: history, meta-analysis and recommendations. *Journal of Applied Ichthyology* **22**, 241–253. doi:10.1111/j.1439-0426.2006.00805.x.
- Fuglstad, G.A., Lindgren, F., Simpson, D. and Rue, H. (2015) Exploring a new class of non-stationary spatial Gaussian random fields with varying local anisotropy. *Statistica Sinica* **25**, 115–133.
- Fuglstad, G.A., Simpson, D., Lindgren, F. and Rue, H. (2019) Constructing priors that penalize the complexity of Gaussian random fields. *Journal of the American Statistical Association* **114**, 445–452. doi:10.1080/01621459.2017.1415907.
- Grüss, A., Gao, J., Thorson, J., Rooper, C., Thompson, G., Boldt, J. and Lauth, R. (2020) Estimating synchronous changes in condition and density in eastern Bering Sea fishes. *Marine Ecology Progress Series* **635**, 169–185. doi:10.3354/meps13213.

- Grüss, A., Gao, J., Thorson, J., Rooper, C., Thompson, G., Boldt, J. and Lauth, R. (2020) Estimating synchronous changes in condition and density in eastern Bering Sea fishes. *Marine Ecology Progress Series* **635**, 169–185. doi:10.3354/meps13213.
- Gubiani, É.A., Ruaro, R., Ribeiro, V.R. and Fé, Ú.M.G.D.S. (2020) Relative condition factor: Le Cren’s legacy for fisheries science. *Acta Limnologica Brasiliensia* **32**, e3. doi:10.1590/s2179-975x13017.
- Haltuch, M., Brooks, E., Brodziak, J., Devine, J. *et al.* (2019) Unraveling the recruitment problem: A review of environmentally-informed forecasting and management strategy evaluation. *Fisheries Research* **217**, 198–216. doi:10.1016/j.fishres.2018.12.016.
- Heintz, R.A., Siddon, E.C., Farley, E.V. and Napp, J.M. (2013) Correlation between recruitment and fall condition of age-0 pollock (*Theragra chalcogramma*) from the eastern Bering Sea under varying climate conditions. *Deep Sea Research Part II: Topical Studies in Oceanography* **94**, 150–156. doi:10.1016/j.dsr2.2013.04.006.
- Hoffman, M.D. and Gelman, A. (2014) The No-U-Turn Sampler: adaptively setting path lengths in Hamiltonian Monte Carlo. *Journal of Machine Learning Research* **15**, 1593–1623.
- Indivero, J., Essington, T.E., Ianelli, J.N. and Thorson, J.T. (2023) Incorporating distribution shifts and spatio-temporal variation when estimating weight-at-age for stock assessments: a case study involving the Bering Sea pollock (*Gadus chalcogrammus*). *ICES Journal of Marine Science* **80**, 258–271. doi:10.1093/icesjms/fsac236.
- IPHC (2024) *IPHC Fishery-Independent Setline Survey Sampling Manual (2024)*. URL <https://www.iphc.int/research/design-and-implementation/>.
- Johnson, K.F., Monnahan, C.C., McGilliard, C.R., Vert-pre, K.A. *et al.* (2015) Time-varying natural mortality in fisheries stock assessment models: Identifying a default approach. *ICES Journal of Marine Science* **72**, 137–150. doi:10.1093/icesjms/fsu055.
- Keller, A.A., Ciannelli, L., Wakefield, W.W., Simon, V., Barth, J.A. and Pierce, S.D. (2017) Species-specific responses of demersal fishes to near-bottom oxygen levels within the California Current large marine ecosystem. *Marine Ecology Progress Series* **568**, 151–173. doi:10.3354/meps12066.
- Krishka, B.A., Starr, P.J. and Choromanski, E.M. (2005) Longspine thornyhead random stratified trawl survey off the west coast of Vancouver Island, September 4-21, 2003. *Can. Tech. Rep. Fish. Aquat. Sci.* **2577**, vi + 93 p. URL <https://publications.gc.ca/site/eng/422422/publication.html>.
- Kristensen, K., Nielsen, A., Berg, C.W., Skaug, H. and Bell, B.M. (2016) TMB: Automatic Differentiation and Laplace Approximation. *J. Stat. Softw.* **70**, 1–21. doi:10.18637/jss.v070.i05.
- Lacko, L., Acheson, S. and Holt, K. (2023) Summary of the annual 2021 Sablefish (*Anoplopoma fimbria*) trap survey, October 6 - November 21, 2021. *Can. Tech. Rep. Fish. Aquat. Sci.* **353**, vii + 48 p.
- Lambert, Y. and Dutil, J.D. (1997) Condition and energy reserves of Atlantic cod (*Gadus morhua*) during the collapse of the northern Gulf of St. Lawrence stock. *Canadian Journal of Fisheries and Aquatic Sciences* **54**, 2388–2400. doi:10.1139/f97-145.
- Le Cren, E.D. (1951) The Length-Weight Relationship and Seasonal Cycle in Gonad Weight and Condition in the Perch (*Perca fluviatilis*). *The Journal of Animal Ecology* **20**, 201. doi:10.2307/1540.

- Legault, C.M. and Palmer, M.C. (2015) In what direction should the fishing mortality target change when natural mortality increases within an assessment? *Canadian Journal of Fisheries and Aquatic Sciences* **73**, 349–357. doi:10.1139/cjfas-2015-0232.
- Levin, L.A. and Le Bris, N. (2015) The deep ocean under climate change. *Science* **350**, 766–768. doi:10.1126/science.aad0126.
- Lindgren, F. (2024) *fmeshes: Triangle Meshes and Related Geometry Tools*. R package version 0.2.0.
- Lindgren, F., Rue, H. and Lindström, J. (2011) An explicit link between Gaussian fields and Gaussian Markov random fields: The stochastic partial differential equation approach. *Journal of the Royal Statistical Society: Series B (Statistical Methodology)* **73**, 423–498. doi:10.1111/j.1467-9868.2011.00777.x.
- Lindmark, M., Anderson, S.C., Gogina, M. and Casini, M. (2023) Evaluating drivers of spatiotemporal variability in individual condition of a bottom-associated marine fish, Atlantic cod (*Gadus morhua*). *ICES Journal of Marine Science* **80**, 1539–1550. doi:10.1093/icesjms/fsad084.
- Lindmark, M., Ohlberger, J. and Gårdmark, A. (2022) Optimum growth temperature declines with body size within fish species. *Global Change Biology* **28**, 2259–2271. doi:10.1111/gcb.16067.
- Litzow, M.A., Hunsicker, M.E., Ward, E.J., Anderson, S.C. *et al.* (2020) Evaluating ecosystem change as gulf of alaska temperature exceeds the limits of preindustrial variability. *Progress in Oceanography* **186**, 102393. doi:https://doi.org/10.1016/j.pocean.2020.102393.
- Lloret, J. (2002) Effects of large-scale habitat variability on condition of demersal exploited fish in the north-western Mediterranean. *ICES Journal of Marine Science* **59**, 1215–1227. doi:10.1006/jmsc.2002.1294.
- Love, M.S. (2011) *Certainly more than you want to know about the fishes of the Pacific Coast: a postmodern experience*. Really Big Press.
- Marentette, J.R. and Kronlund, A.R. (2020) Cross-Jurisdictional Review of International Fisheries Policies, Standards and Guidelines: Considerations for a Canadian Science Sector Approach. Technical Report Can. Tech. Rep. Fish. Aquat. Sci. 3342.
- Marshall, C.T. and Frank, K.T. (1999) The effect of interannual variation in growth and condition on haddock recruitment. *Canadian Journal of Fisheries and Aquatic Sciences* **56**, 347–355. doi:10.1139/f99-019.
- Marshall, C.T., Yaragina, N.A., Lambert, Y. and Kjesbu, O.S. (1999) Total lipid energy as a proxy for total egg production by fish stocks. *Nature* **402**, 288–290. doi:10.1038/46272.
- Mason, J.G., Weisberg, S.J., Morano, J.L., Bell, R.J. *et al.* (2023) Linking knowledge and action for climate-ready fisheries: Emerging best practices across the US. *Marine Policy* **155**, 105758. doi:10.1016/j.marpol.2023.105758.
- Maunder, M.N. and Thorson, J.T. (2019) Modeling temporal variation in recruitment in fisheries stock assessment: A review of theory and practice. *Fisheries Research* **217**, 71–86. doi:10.1016/j.fishres.2018.12.014.
- McCullagh, P. and Nelder, J.A. (1989) *Generalized linear models*. Chapman & Hall, New York.
- Michalsen, K. (1998) Growth of North-east Arctic cod (*Gadus morhua*L.) in relation to ambient temperature. *ICES Journal of Marine Science* **55**, 863–877. doi:10.1006/jmsc.1998.0364.

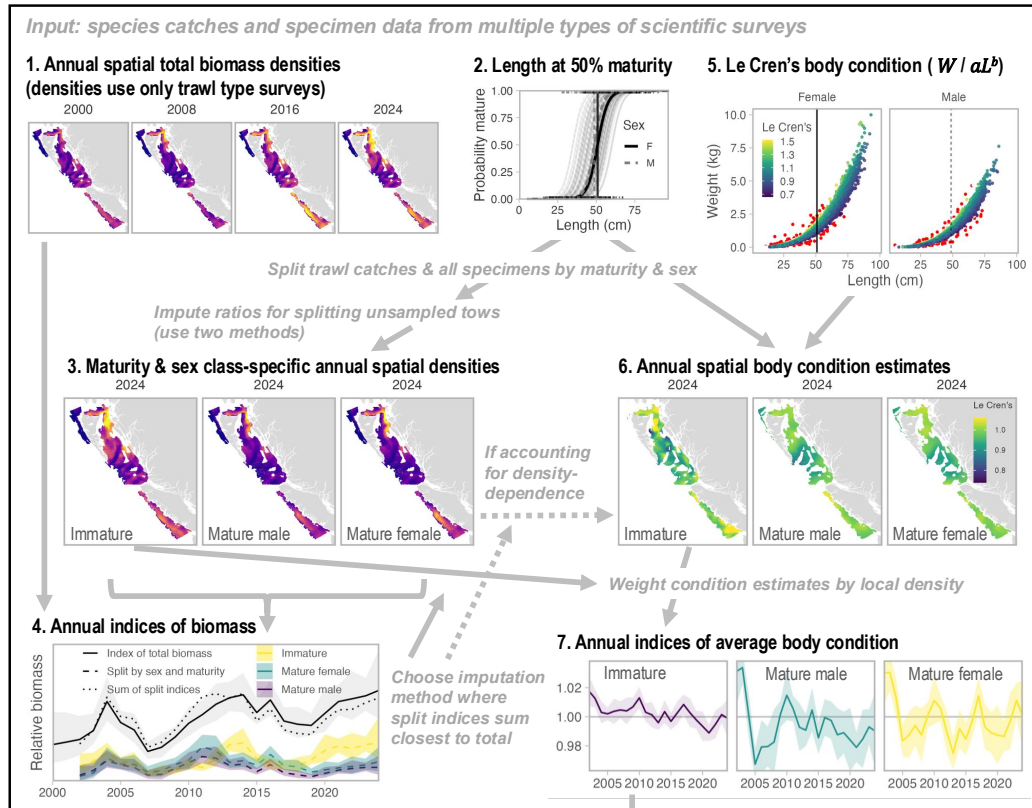
- Morgan, M.J. (2004) The relationship between fish condition and the probability of being mature in American plaice (*Hippoglossoides platessoides*). *ICES Journal of Marine Science* **61**, 64–70. doi:10.1016/j.icesjms.2003.09.001.
- Myers, R.A., Barrowman, N.J. and Thompson, K.R. (1995) Synchrony of recruitment across the north atlantic: an update. (or, “now you see it, now you don’t!”). *ICES Journal of Marine Science* **52**, 103–110. doi:10.1016/1054-3139(95)80019-0.
- Myers, R.A. (1998) When do environment-recruitment correlations work? *Reviews in Fish Biology and Fisheries* **8**, 285–305. doi:10.1023/A:1008828730759.
- Nottingham, M.K., Williams, D.C., Wyeth, M.R. and Olsen, N. (2017) Summary of the West Coast Vancouver Island synoptic bottom trawl survey, May 28 – June 21, 2014. *DFO Can. Manuscr. Rep. Fish. Aquat. Sci.* **2017/3140**, viii + 55 p.
- Peig, J. and Green, A.J. (2009) New perspectives for estimating body condition from mass/length data: The scaled mass index as an alternative method. *Oikos* **118**, 1883–1891. doi:10.1111/j.1600-0706.2009.17643.x.
- Peig, J. and Green, A.J. (2010) The paradigm of body condition: a critical reappraisal of current methods based on mass and length. *Functional Ecology* **24**, 1323–1332. doi:10.1111/j.1365-2435.2010.01751.x.
- Pepin, P., King, J., Holt, C., Gurney-Smith, H., Shackell, N., Hedges, K. and Bundy, A. (2022) Incorporating knowledge of changes in climatic, oceanographic and ecological conditions in Canadian stock assessments. *Fish and Fisheries* **23**, 1332–1346. doi:10.1111/faf.12692.
- Peña, M.A., Fine, I. and Callendar, W. (2019) Interannual variability in primary production and shelf-offshore transport of nutrients along the northeast Pacific Ocean margin. *Deep Sea Research Part II: Topical Studies in Oceanography* **169–170**, 104637. doi:10.1016/j.dsr2.2019.104637.
- Pinsky, M.L., Worm, B., Fogarty, M.J., Sarmiento, J.L. and Levin, S.A. (2013) Marine taxa track local climate velocities. *Science* **341**, 1239–1242. doi:10.1126/science.1239352.
- Punt, A.E., A’mar, T., Bond, N.A., Butterworth, D.S. *et al.* (2014) Fisheries management under climate and environmental uncertainty: Control rules and performance simulation. *ICES Journal of Marine Science* **71**, 2208–2220. doi:10.1093/icesjms/fst057.
- Punt, A.E., Castillo-Jordán, C., Hamel, O.S., Cope, J.M., Maunder, M.N. and Ianelli, J.N. (2021) Consequences of error in natural mortality and its estimation in stock assessment models. *Fisheries Research* **233**, 105759. doi:10.1016/j.fishres.2020.105759.
- R Core Team (2024) *R: A Language and Environment for Statistical Computing*. R Foundation for Statistical Computing, Vienna, Austria. URL <https://www.R-project.org/>.
- Rätz, H.J. and Lloret, J. (2003) Variation in fish condition between Atlantic cod (*Gadus morhua*) stocks, the effect on their productivity and management implications. *Fisheries Research* **60**, 369–380. doi:10.1016/S0165-7836(02)00132-7.
- Ray, C. and Hastings, A. (1996) Density Dependence: Are We Searching at the Wrong Spatial Scale? *Journal of Animal Ecology* **65**, 556–566. doi:10.2307/5736.
- Regular, P.M., Buren, A.D., Dwyer, K.S., Cadigan, N.G. *et al.* (2022) Indexing starvation mortality to assess its role in the population regulation of Northern cod. *Fisheries Research* **247**, 106180. doi:10.1016/j.fishres.2021.106180.

- Ricker, W.E. (1954) Stock and Recruitment. *Journal of the Fisheries Research Board of Canada* **11**, 559–623. doi:10.1139/f54-039.
- Rindorf, A., Van Deurs, M., Howell, D., Andonegi, E. *et al.* (2022) Strength and consistency of density dependence in marine fish productivity. *Fish and Fisheries* **23**, 812–828. doi:10.1111/faf.12650.
- Robinson, C., Bertram, D., Shannon, H., Von Biela, V., Greentree, W., Duguid, W. and Arimitsu, M. (2024) Reduction in overwinter body condition and size of Pacific sand lance has implications for piscivorous predators during marine heatwaves. *Marine Ecology Progress Series* **737**, 89–99. doi:10.3354/meps14257.
- Roux, M.J., Duplisea, D.E., Hunter, K.L. and Rice, J. (2022) Consistent Risk Management in a Changing World: Risk Equivalence in Fisheries and Other Human Activities Affecting Marine Resources and Ecosystems. *Frontiers in Climate* **3**, 781559. doi:10.3389/fclim.2021.781559.
- Sinclair, A., Schnute, J., Haigh, R., Starr, P., Stanley, R., Fargo, J. and Workman, G. (2003) Feasibility of multispecies groundfish trawl surveys on the BC coast. *DFO Can. Sci. Adv. Sec. Res. Doc.* **2003/049**, i + 34 p.
- Sinclair, A. and Workman, G. (2002) A review of Pacific cod (*Gadus macrocephalus*) monitoring surveys in Hecate Strait, March–July 2002. *DFO Can. Sci. Adv. Sec. Res. Doc.* **2002/130**, 59 p.
- Somov, A., Farley, E.V., Yasumiishi, E.M. and McPhee, M.V. (2024) Comparison of Juvenile Pacific Salmon abundance, distribution, and body condition between Western and Eastern Bering Sea using spatiotemporal models. *Fisheries Research* **278**, 107086. doi:10.1016/j.fishres.2024.107086.
- Stan Development Team (2022) RStan: the R interface to Stan. URL <https://mc-stan.org/>. R package version 2.21.5.
- Starr, P.J., Krishka, B.A. and Choromanski, E.M. (2002) Trawl survey for thornyhead biomass estimation off the west coast of Vancouver Island, September 15 to October 2, 2001. *Can. Tech. Rep. Fish. Aquat. Sci.* **2421**, 60 p. URL <https://publications.gc.ca/site/eng/422422/publication.html>.
- Stawitz, C., Haltuch, M. and Johnson, K. (2019) How does growth misspecification affect management advice derived from an integrated fisheries stock assessment model? *Fisheries Research* **213**, 12–21. doi:10.1016/j.fishres.2019.01.004.
- Szuwalski, C.S. and Hollowed, A.B. (2016) Climate change and non-stationary population processes in fisheries management. *ICES Journal of Marine Science* **73**, 1297–1305. doi:10.1093/icesjms/fsv229.
- Tamburello, N., Connors, B.M., Fullerton, D. and Phillis, C.C. (2019) Durability of environment–recruitment relationships in aquatic ecosystems: Insights from long-term monitoring in a highly modified estuary and implications for management. *Limnology and Oceanography* **64**. doi:10.1002/lno.11037.
- Thompson, P.L., Nephin, J., Davies, S.C., Park, A.E. *et al.* (2023) Groundfish biodiversity change in northeastern Pacific waters under projected warming and deoxygenation. *Philosophical Transactions of the Royal Society B: Biological Sciences* **378**, 20220191. doi:10.1098/rstb.2022.0191.
- Thorson, J.T., Cunningham, C.J., Jorgensen, E., Havron, A., Hulson, P.J.F., Monnahan, C.C. and von Szalay, P. (2021) The surprising sensitivity of index scale to delta-model assumptions: Recommendations for model-based index standardization. *Fisheries Research* **233**, 105745. doi:10.1016/j.fishres.2020.105745.

- Thorson, J.T. and Kristensen, K. (2016) Implementing a generic method for bias correction in statistical models using random effects, with spatial and population dynamics examples. *Fisheries Research* **175**, 66–74. doi:10.1016/j.fishres.2015.11.016.
- Thorson, J.T., Shelton, A.O., Ward, E.J. and Skaug, H.J. (2015a) Geostatistical delta-generalized linear mixed models improve precision for estimated abundance indices for West Coast groundfishes. *ICES J. Mar. Sci.* **72**, 1297–1310. doi:10.1093/icesjms/fsu243.
- Thorson, J.T., Skaug, H.J., Kristensen, K., Shelton, A.O., Ward, E.J., Harms, J.H. and Benante, J.A. (2015b) The importance of spatial models for estimating the strength of density dependence. *Ecology* **96**, 1202–1212. doi:10.1890/14-0739.1.
- Thorson, J. (2015) Spatio-temporal variation in fish condition is not consistently explained by density, temperature, or season for California Current groundfishes. *Marine Ecology Progress Series* **526**, 101–112. doi:10.3354/meps11204.
- Tweedie, M.C.K. (1984) An index which distinguishes between some important exponential families. In: *Statistics: Applications and New Directions. Proceedings of the Indian Statistical Institute Golden Jubilee International Conference* (eds. J.K. Gosh and J. Roy). Indian Statistical Institute, Calcutta, pp. 579–604.
- Van Deurs, M., Jacobsen, N.S., Behrens, J.W., Henriksen, O. and Rindorf, A. (2023) The interactions between fishing mortality, age, condition and recruitment in exploited fish populations in the North Sea. *Fisheries Research* **267**, 106822. doi:10.1016/j.fishres.2023.106822.
- Vehtari, A., Gelman, A., Simpson, D., Carpenter, B. and Bürkner, P.C. (2021) Rank-normalization, folding, and localization: An improved  $\hat{R}$  for assessing convergence of mcmc (with discussion). *Bayesian Analysis* **16**, 667–718. doi:10.1214/20-BA1221.
- Ward, E.J., Anderson, S.C., Damiano, L.A., Hunsicker, M.E. and Litzow, M.A. (2019) Modeling regimes with extremes: the bayesdfa package for identifying and forecasting common trends and anomalies in multivariate time-series data. *The R Journal* **11**, 46–55. doi:10.32614/RJ-2019-007.
- Whitten, A.R., Klaer, N.L., Tuck, G.N. and Day, R.W. (2013) Accounting for cohort-specific variable growth in fisheries stock assessments: A case study from south-eastern Australia. *Fisheries Research* **142**, 27–36. doi:10.1016/j.fishres.2012.06.021.
- Williams, D.C., Nottingham, M.K., Olsen, N. and Wyeth, M.R. (2018a) Summary of the Queen Charlotte Sound synoptic bottom trawl survey, July 6 – August 8, 2015. *DFO Can. Manuscr. Rep. Fish. Aquat. Sci.* **3136**, viii + 64 p.
- Williams, D.C., Nottingham, M.K., Olsen, N. and Wyeth, M.R. (2018b) Summary of the West Coast Haida Gwaii synoptic bottom trawl survey, August 25 – October 2, 2014. *DFO Can. Manuscr. Rep. Fish. Aquat. Sci.* **2018/3134**, viii + 42 p.
- Wuenschel, M.J., McElroy, W.D., Oliveira, K. and McBride, R.S. (2019) Measuring fish condition: an evaluation of new and old metrics for three species with contrasting life histories. *Canadian Journal of Fisheries and Aquatic Sciences* **76**, 886–903. doi:10.1139/cjfas-2018-0076.
- Wyeth, M.R., Olsen, N., Nottingham, M.K. and Williams, D.C. (2018) Summary of the Hecate Strait synoptic bottom trawl survey, May 26 – June 22, 2015. *DFO Can. Manuscr. Rep. Fish. Aquat. Sci.* **2018/3126**, viii + 55 p.

## 9 Figures

## Species-level analyses



## Ecosystem-level analyses

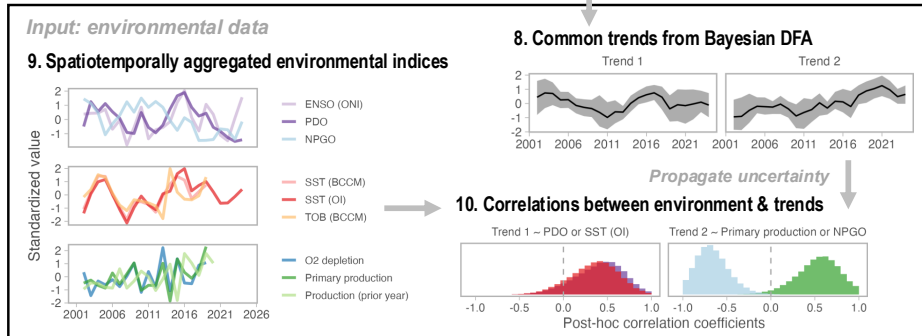


Figure 1: Diagram of how the steps in this analysis link together. Analytical outputs are labelled in black and illustrated. Inputs and intervening steps are described using grey arrows and italics. Dashed arrows apply only when adjusting condition indices to exclude effects of density-dependence (not illustrated). Species-level outputs are for Pacific Cod (*Gadus macrocephalus*) and ecosystem-level ones are for immature indices. All steps rely on data from trawl, longline, and trap surveys (unless otherwise stated). Steps 3 and 6 are from spatiotemporal models that estimate independent distributions for each maturity and sex class. Steps 4 and 7 use spatial estimates to generate annual indices of abundance. Step 8 combines results of step 7 from all species. Step 6 on can be conducted either with, or without, excluding effects of density-dependence. Steps 9 and 10 aggregate environment variables and compare these with trends from step 8 using Bayesian posthoc correlation tests to propagate trend uncertainty.

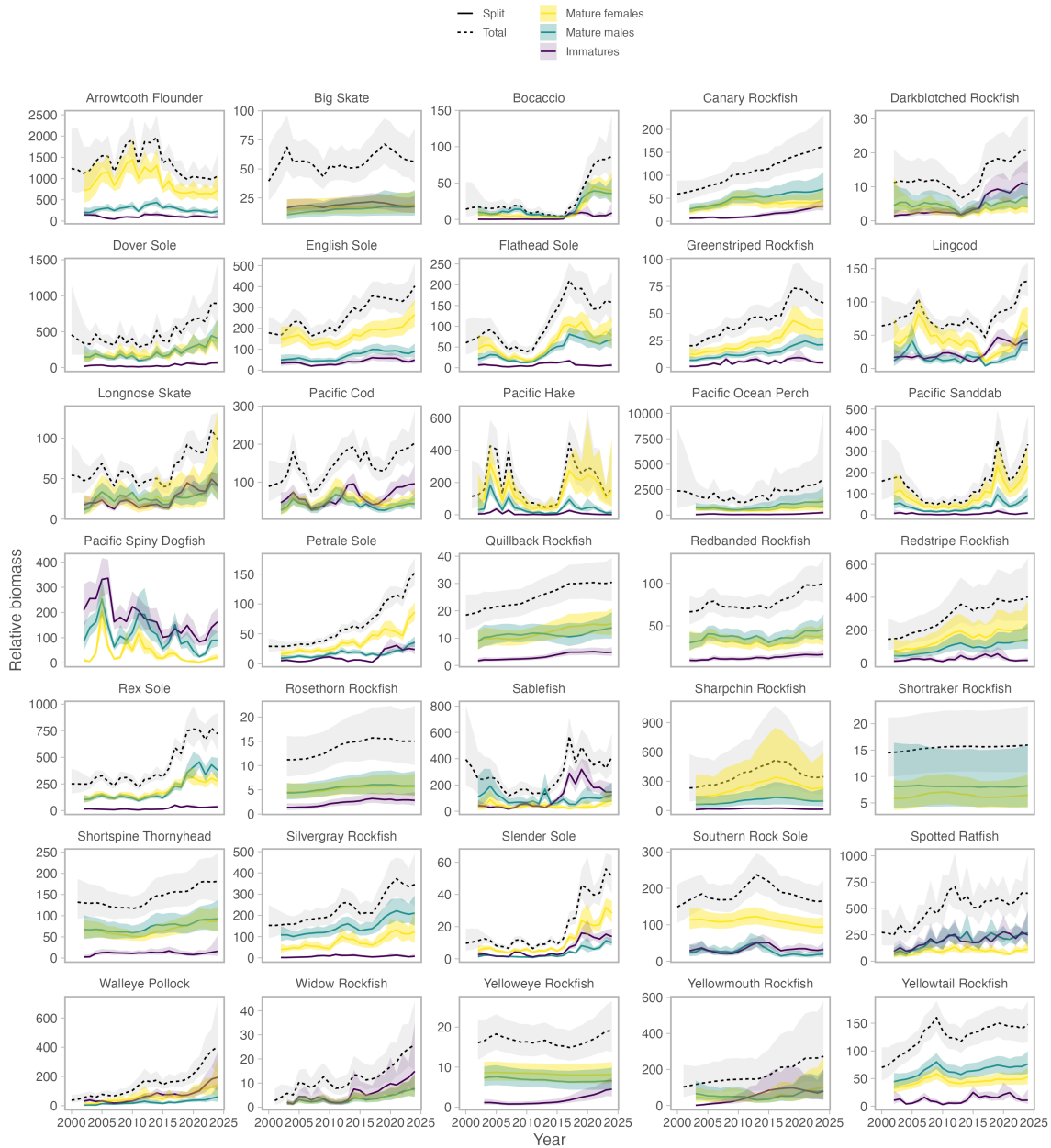


Figure 2: Annual Canadian biomass indices for each maturity class and overall for 35 species of Pacific groundfish. Represents combined biomass for all synoptic trawl survey grids on the summer solstice and scaled in tonnes. Each index was modelled independently from the data subset (‘all catches’ vs. ‘sampled catches’ see ‘Supporting Methods: Decision rules for splitting total catches from unsampled tows’) for which the indices for all three maturity classes (solid coloured lines) summed to match most closely the total index (dotted line).

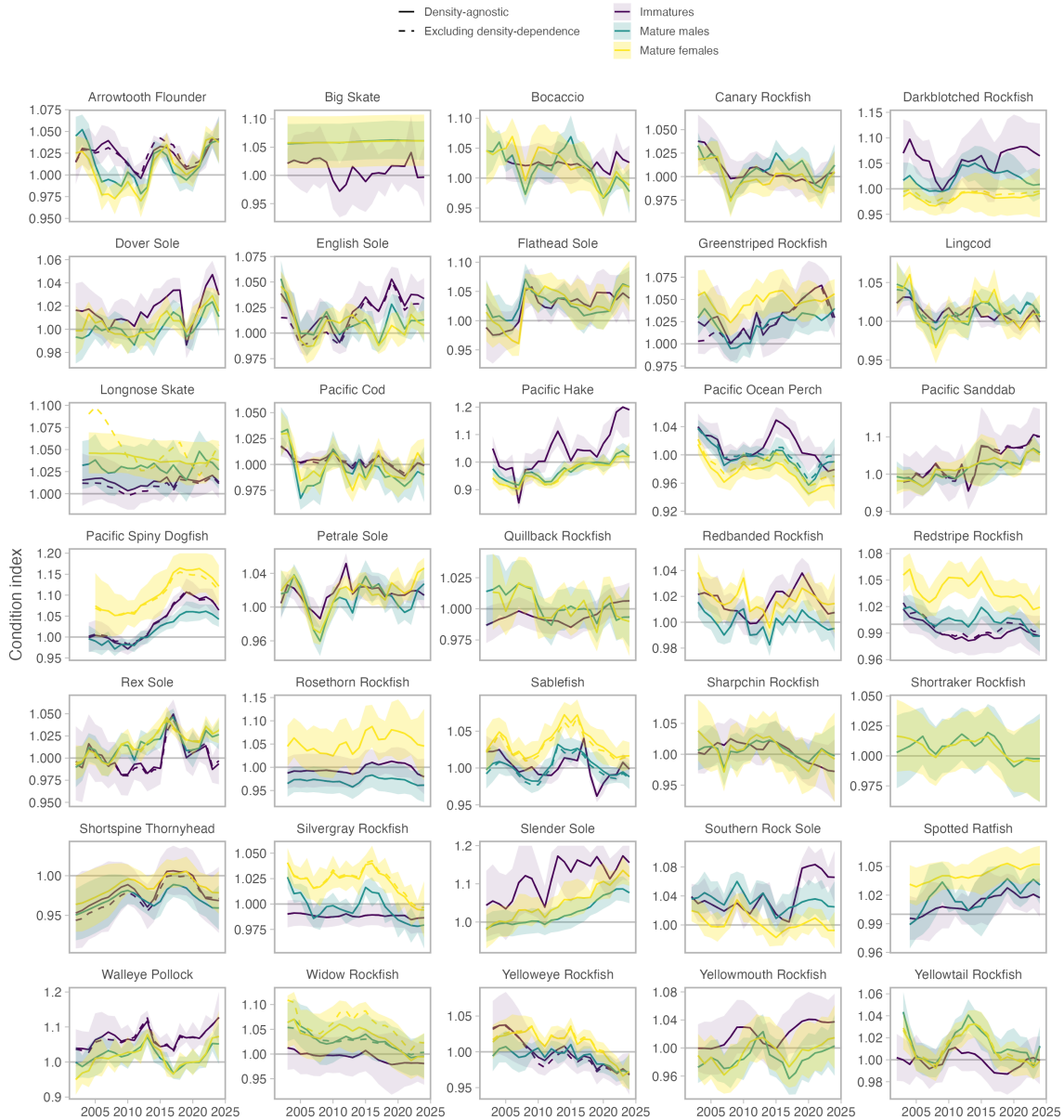


Figure 3: Annual indices of Le Cren’s body condition for each maturity class for 35 species of Pacific groundfish. These represent Canadian coastwide averages, weighted by the same local biomass estimates used to generate the biomass indices in Figure 2. Solid lines represent modelled population predictions, while dashed lines represent the average condition adjusted to exclude any estimated negative effects of local biomass density.

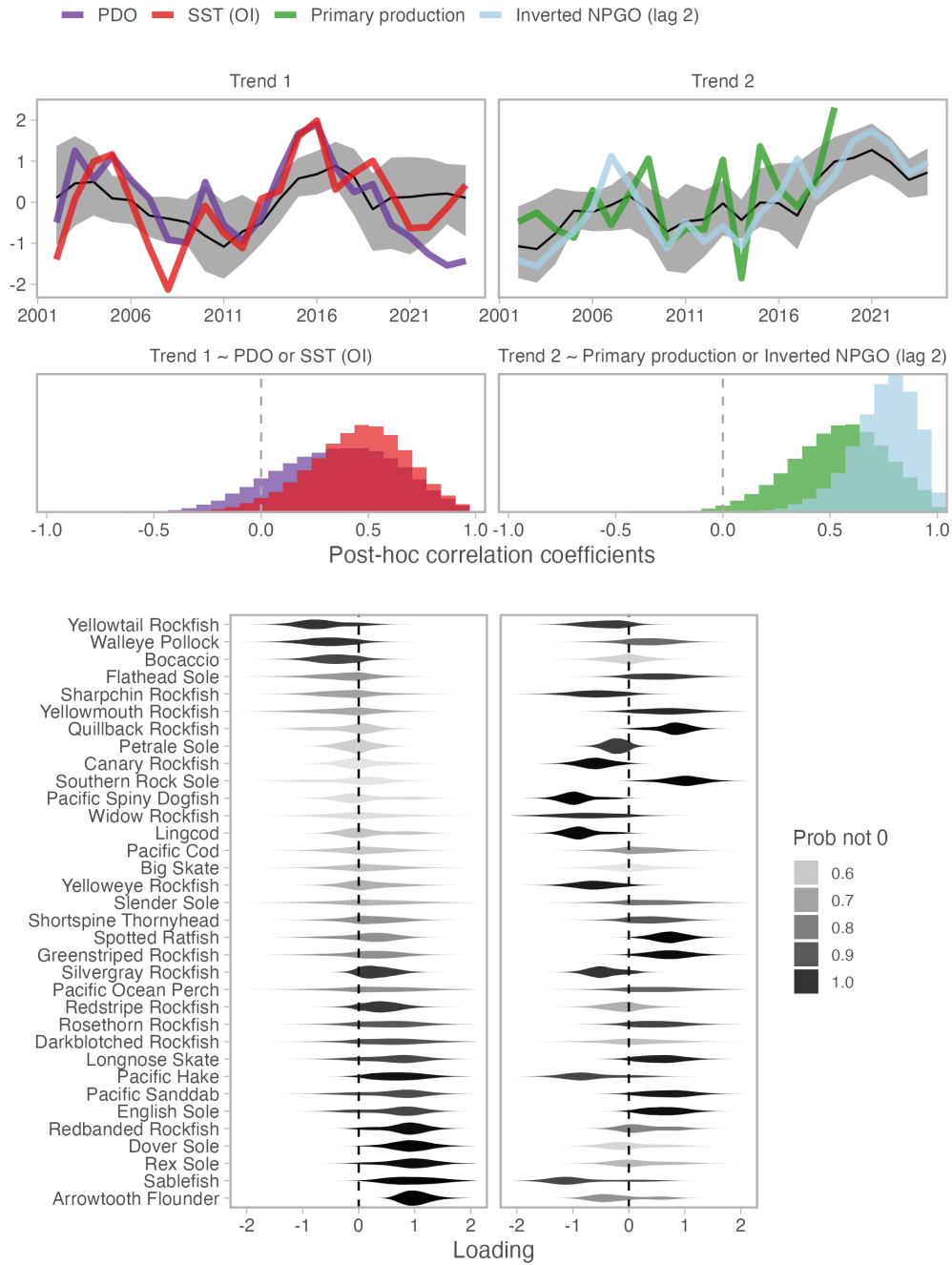


Figure 4: Common trends in immature body condition after accounting for negative effects of local biomass density (top row) are most correlated with both SST and PDO (trend 1) and NPGO two years prior or current season primary production (trend 2) as indicated by histograms of post-hoc correlation coefficients (middle row). All environmental covariates were standardized and NPGO was inverted for easier comparison with primary production. Shading on violin plots indicate how different from zero the posterior for each loading is (bottom plot). Species with a strong positive relationship with a given trend have dark violins on the right of the dashed lines; those with strong negative relationships have dark violins to the left of the dashed lines.

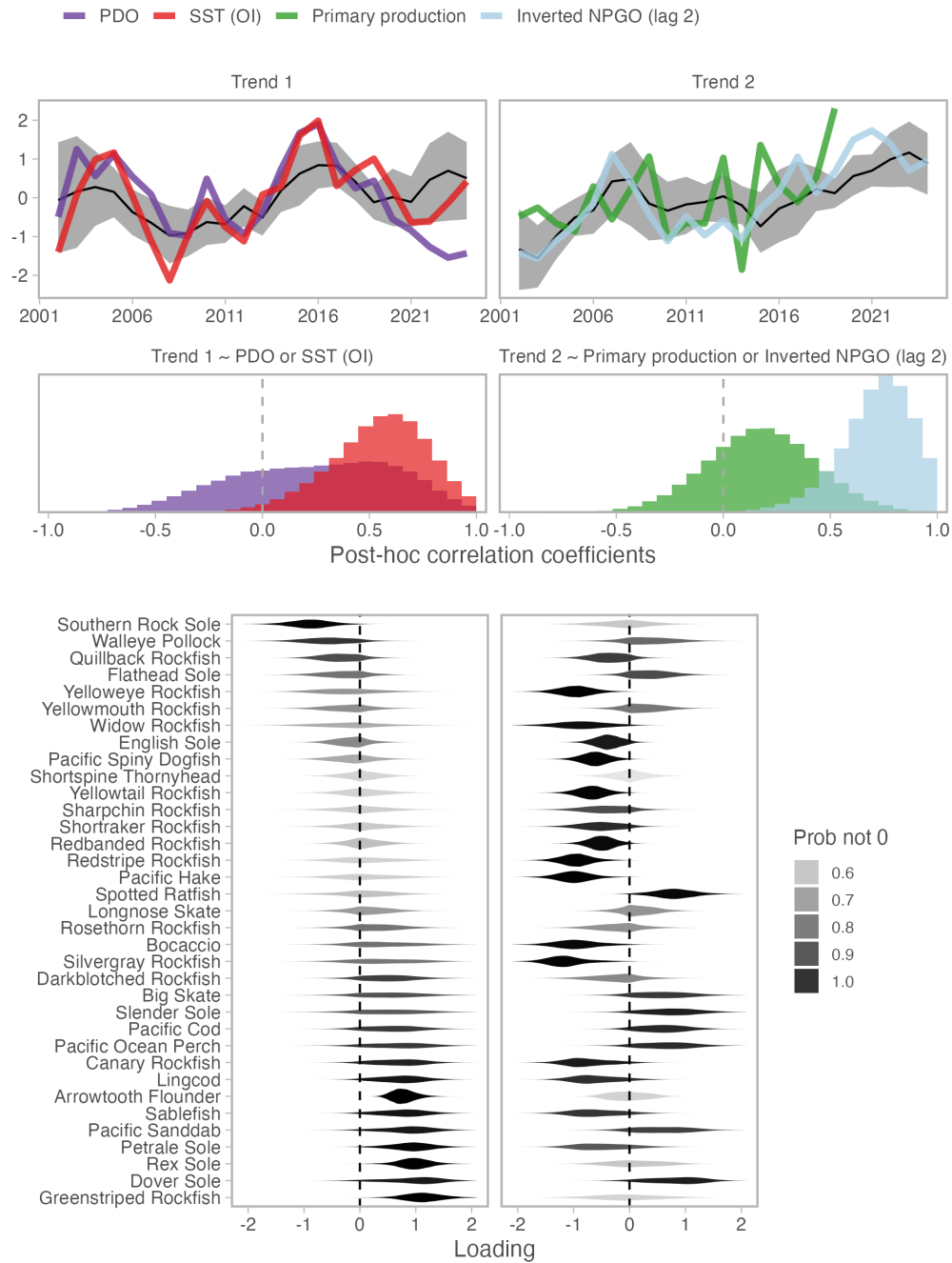


Figure 5: Common trends in mature male body condition after accounting for negative effects of local biomass density (top row) are most correlated with SST (trend 1) and with NPGO (trend 2) as indicated by histograms of post-hoc correlation coefficients (middle row). Correlations with PDO and primary production are much weaker than for immatures (Figure 4). Covariates and panels as described in caption for Figure 4.

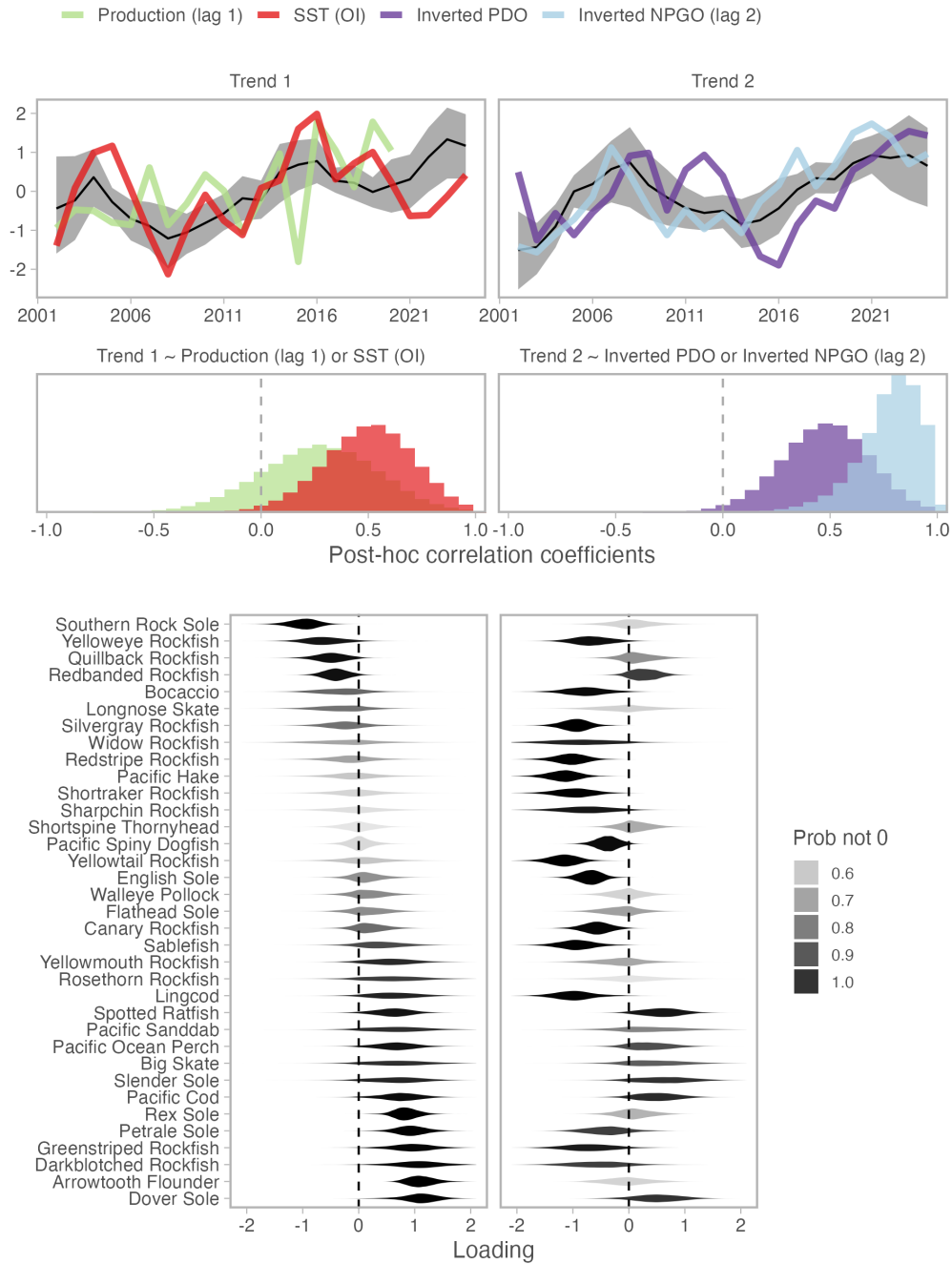


Figure 6: Common trends in mature female body condition after accounting for negative effects of local biomass density (top row) are correlated with current year SST and more weakly with previous year primary production (trend 1) and both with current year NPGO and PDO (trend 2) as indicated by histograms of post-hoc correlation coefficients (middle row). Covariates and panels as described in caption for Figure 4 though PDO has been inverted here to match orientation of trend 2.

Supporting Materials: Body condition as a shared response to  
environment in a commercially important demersal fish  
assemblage

Philina A. English<sup>1</sup>, Sean C. Anderson<sup>1,2</sup>, and Robyn E. Forrest<sup>1</sup>

<sup>1</sup>Pacific Biological Station, Fisheries and Oceans Canada, Nanaimo, BC, Canada

<sup>2</sup>School of Resource and Environmental Management, Simon Fraser University,  
Burnaby, BC, Canada

\*corresponding author: [ecophilina@gmail.com](mailto:ecophilina@gmail.com)

# A Supporting methods

## 2 A.1 Fishery-independent survey data

A variety of gear types are used to conduct fishery-independent surveys in Canada’s Pacific waters. Spatial coverage is also highly variable, generally with biennial coverage of each region (Figures S1, S2). To maximize the sample size and spatiotemporal representation, we used morphological measurements collected from fishery-independent surveys using a variety of gear types, and total catch weights from any trawl survey where at least 1% of all sets between 2000 and 2024, and at least 3 years and half of years when the survey was conducted, had positive sets for a species. In all surveys, protocols for collecting individual-level data varied among species, depending on size of catch, scientific interest, and commercial importance of the species. In general, fish were individually weighed, measured, and sexed for catches of between 10–50 fish, while larger catches were sub-sampled. For commercially important species, additional data on reproductive maturity and hard structures for ageing (otoliths, fin sections) were also collected. Data from surveys conducted in the waters inside Vancouver Island were excluded, because for some species the populations occupying these areas are considered distinct.

### 16 A.1.1 Synoptic bottom trawl surveys

Four contemporary synoptic bottom trawl surveys (SYN) target groundfish over soft bottom habitats at depths between 10 and 1,300 m (Anderson *et al.* 2019). Combined they cover most of the upper continental slope and shelf in Pacific Canada. These surveys are stratified within four regions, two of which are usually surveyed in odd years (Hecate Strait and Queen Charlotte Sound) and two in even years (West Coast Vancouver Island and West Coast Haida Gwaii). Each region was sampled over the same month-long period between late May and early August in each survey year. These surveys share similar random depth-stratified designs, fishing gear and fishing protocols (Sinclair *et al.* 2003, Nottingham *et al.* 2017, Wyeth *et al.* 2018, Williams *et al.* 2018a,b).

### A.1.2 Other trawl surveys

26 For estimating biomass density, we also used data from four other trawl surveys, which occurred in different years and had somewhat different sampling designs to the synoptic surveys (e.g., some used 28 fixed stations and/or sampled different depth strata). The models in our analysis used random walk spatiotemporal Gaussian Markov random fields, estimated catchability intercepts for each survey 30 type, a depth covariate, and area sampled calculations (see ‘Effort calculation for trawl surveys’), therefore allowing us to use these other surveys to help bridge the biennial sampling structure of the 32 synoptic surveys.

In the few years immediately prior to the full implementation of the four synoptic surveys, 34 three surveys collected abundance and morphological data for a variety of groundfish species within narrower depth ranges. The Hecate Strait Multispecies Assemblage Survey (MSA) had a fixed-station design that was depth-stratified between 20 and 200 m (Choromanski *et al.* 2005). This survey 36 was conducted approximately biennially between 1984 and 2003 (though occurred in 2000, 2002 and

38 2003), but morphological measurements were only collected starting in 1998. The Hecate Strait  
Pacific Cod (*Gadus macrocephalus*) survey (HS PCOD) targeted known hotspots for this species  
40 annually for three years (2002-2004; Sinclair and Workman 2002). The depths sampled ranged from  
22 to 168 m. Abundance data was collected for all groundfish species encountered, but morphological  
42 data was collected only for the target species and Pacific Halibut (*Hippoglossus stenolepis*; hereafter  
'halibut'). The West Coast Vancouver Island Thornyhead Bottom Trawl (THORNYHEAD) used a  
44 stratified random design targeting depths between 500 and 1600 m annually for three years (2001-  
2003; Starr *et al.* 2002, Krishka *et al.* 2005).

46 The Multispecies Small-mesh Bottom Trawl Survey (MSSM) targets shrimp, but also catches  
groundfish. This survey has been conducted off the west coast of Vancouver Island most years since  
48 1975 and in Queen Charlotte Sound between 1998 and 2016. This survey currently follows a fixed  
station design covering depths mostly between 50 and 200 m, but it has undergone some changes  
50 since its inception. In our species distribution models, we account for a gear change in 2006 by  
including different catchabilities before and after this change (Dunic and Anderson 2025).

52 Integrated acoustic-trawl surveys (HAKE) targeting Pacific Hake (*Merluccius productus*) have  
been conducted in Canadian waters since 1977 (de Blois 2020). This survey uses echosounders to  
54 detect likely schools of Pacific Hake and then tows a net to sample these schools for species and  
size composition. Overall, tows from the Hake survey are sparse across much of the coast in most  
56 years, but are especially useful for schooling rockfish and Gadiformes that frequently occur further  
up in the water column (e.g., Walleye Pollock, *Gadus chalcogrammus*; Pacific Ocean Perch, *Sebastes*  
58 *alutus*; Yellowtail Rockfish, *Sebastes flavidus*). Lengths, and sometimes weights, were taken from all  
rockfish and any species that was dominant in the catch composition.

### 60 A.1.3 Longline and trap surveys

Three longline hook surveys and one trap survey are also conducted in Canada's Pacific shelf and  
62 slope waters. These surveys were not used for calculating biomass density because the catches were  
recorded in numbers rather than weight and area swept estimates are harder to generate. However,  
64 biological sample data from these surveys were used in estimation of length-weight relationships,  
length at maturity, and body condition. In addition to other targeted species, these surveys col-  
66 lected morphological measurements for most rockfish species, and starting in 2018 lingcod (*Ophiodon*  
*elongatus*) as well.

68 The Outside Hard Bottom Longline surveys (HBLL) are conducted biennially beginning in 2006  
for the northern region and 2007 for the southern region (Anderson *et al.* 2019, Doherty *et al.* 2019).  
70 These surveys targeted hard-bottom habitats in untrawlable areas and are of a stratified random  
design with 3 depth strata: shallow (20-70 m), medium (71-150 m) and deep (151-260 m). Rockfish  
72 maturity and length data have been collected from the start of these surveys, with weights recorded  
starting in 2009.

74 The International Pacific Halibut Commission (IPHC) fishery-independent longline survey has a  
fixed station design with stations located at the intersections of an 18.52 km (10 nmi) square grid  
76 intended to span depths ranging from 18-732 m (IPHC 2024). At a randomly selected subset of

these stations, eight skates of 100 ( $\pm 5\%$ ) size 16/0 hooks with 18 ft (5.49 m) spacing between each  
78 hook were set between May 24th and August 26th. Maturity and length data was available for  
halibut starting in 1998, and for most rockfish species since 2003. Weights have been collected for  
80 rockfish since 2009, but were only available for halibut from 2022 and 2023.

The offshore trap surveys targetting sablefish (*Anoplopoma fimbria*) have evolved from fixed  
82 stations (1988 - 2010) to a stratified random design (2003-2023; Lacko *et al.* 2023). The gear  
used consists of a groundline resting on the ocean floor with 25 baited traps attached at 150 foot  
84 intervals and a targeted soak time of 24 hours. Beginning in 2003, maturities, lengths, and weights  
were also collected for Redbanded (*Sebastes babcocki*), Shortraker (*Sebastes borealis*), and Yelloweye  
86 (*Sebastes ruberrimus*) Rockfish. In some years, lengths and weights were also collected for Shortspine  
Thornyhead (*Sebastobus alascanus*), Arrowtooth Flounder (*Atheresthes stomias*), Pacific Spiny  
88 Dogfish (*Squalus suckleyi*), and halibut.

## A.2 Effort calculation for trawl surveys

90 For all trawl surveys, we included only tows that sampled a distance of  $> 500$  m (including those  
that lasted at least 10 minutes and travelled at a speed of at least 50 m per minute). These values  
92 were combined with net opening to estimate the area sampled (e.g., Williams *et al.* 2018a, Anderson  
*et al.* 2019). When the tow-specific value was missing, we applied the mean net opening for that  
94 survey. These values were used to calculate log area swept in  $km^2$  for each tow. This was included  
as an offset in all distribution models (McCullagh and Nelder 1989, p. 206).

## 96 A.3 Decision rules for splitting total catches from unsampled tows

To reduce the risk of highly skewed ratios being the result of very few samples, while retaining as  
98 much spatial and temporal representativeness, we used a threshold of at least six sampled tows (with  
an average of at least three fish measured per tow) as the minimum for a survey-year combination.  
100 These survey-year combinations were defined as having ‘sampled catches’ although some tows were  
not sampled. A lower threshold of 3 sampled tows resulted in some highly skewed proportions  
102 and a higher value of 10 resulted in many cases where realistic proportions were replaced by less  
spatially or temporally relevant values. For unsampled tows in any survey-year combinations that  
104 met this threshold, we applied the average proportion of each class from all sampled tows in that  
survey-year. For unsampled tows in any survey-year combinations with less than this threshold, we  
106 applied the average proportion of each class from all surveys in that year (as long as the average  
SD in proportions across all years within that survey was greater than the SD across all surveys  
108 within each year, and at least six tows were measured in all surveys that year), or for all years for  
each survey (if there were fewer than six tows across all surveys with measurements in that year,  
110 or the average SD in proportions across all years within each survey was less than the SD across  
all surveys within each year). Finally, for surveys with fewer than this threshold over all years, the  
112 global average proportions were applied.

## 114 **A.4 Model convergence and decision rules for simplifying spatiotemporal models**

116 Convergence of spatiotemporal models was determined by checking that the Hessian was positive  
118 definite and the maximum absolute marginal log likelihood gradient with respect to all fixed effects  
120 was  $< 0.005$ . We investigated these thresholds and also checked that all standard errors on fixed  
effects were  $< 100$ , spatial/spatiotemporal range parameters were  $<$  than 1.5 times the greater of the  
maximum latitudinal or longitudinal spread of the data, and that all standard deviation parameters  
were  $> 0.01$  using the `sanity()` function in the `sdmTMB` package (Anderson *et al.* 2024). When  
thresholds were not met, we made the following adjustments to the model.

### 122 **A.4.1 Biomass density models**

124 If the biomass density model had an estimated a range greater than 1.5 times the greater of the  
126 maximum latitudinal or longitudinal spread of the data, we tried sharing the range between the  
spatial and spatiotemporal fields (helpful in  $< 1\%$  of models). If either the standard deviation  
parameters or any standard errors failed to be estimated, we first tried removing the spatial field  
from the second component model (41% of models) and then from both (6% of models). Finally, if  
128 still failing to converge, a Tweedie family model given in Equation 11 was attempted (2% of models  
or 3 of 139). No simplification of the spatial elements was required for Tweedie models.

### 130 **A.4.2 Condition models**

132 When spatiotemporal condition models did not converge, model simplification involved allowing the  
spatial and spatiotemporal fields to share the same range parameter (16% of models), dropping  
anisotropy and adding penalized complexity priors that match those for the density models (16% of  
134 models), or dropping the spatial field entirely when the marginal standard deviation of the spatial  
field when  $\sigma < 0.001$  (61% of models) depending on which components of the model were struggling  
136 to fit. For models that still failed to converge, the prior on range was first doubled, and then  
finally, if that failed, the spatiotemporal field was replaced with a fixed spatial field and a first-order  
138 autoregressive (AR1) intercept on year (4% of models or 4 of 106).

## **Bibliography**

140 Anderson, S., Keppel, E.A. and Edwards, A.M. (2019) A reproducible data synopsis for over 100  
species of British Columbia groundfish. *DFO Can. Sci. Advis. Sec. Res. Doc.* **2019/041**, vii +  
142 321 p.

Anderson, S.C., Ward, E.J., English, P.A., Barnett, L.A.K. and Thorson, J. (2024) `sdmTMB`:  
144 An R package for fast, flexible, and user-friendly generalized linear mixed effects models with  
spatial and spatiotemporal random fields. *In press at Journal of Statistical Software. bioRxiv*  
146 **2022.03.24.485545**. doi:10.1101/2022.03.24.485545.

- 148 Choromanski, E.M., Workman, G. and Fargo, J. (2005) Hecate Strait multispecies bottom trawl  
survey, GGS W.E. Ricker, May 19 to June 7, 2003. *Can. Data Rep. Fish. Aquat. Sci.* **1169**, viii  
+85 p.
- 150 de Blois, S. (2020) The 2019 Joint U.S.–Canada Integrated Ecosystem and Pacific Hake Acoustic-  
Trawl Survey: Cruise Report SH-19-06. *U.S. Department of Commerce, NOAA Processed Report*  
152 **NMFS-NWFSC-PR-2020-03**. URL <https://doi.org/10.25923/p55a-1a22>.
- Doherty, B., Benson, A.J. and P., C.S. (2019) Data summary and review of the PHMA hard bottom  
154 longline survey in British Columbia after the first 10 years (2006-2016). *DFO Can. Tech. Rep.*  
*Fish. Aquat. Sci.* **2019/3276**, ix + 75 p.
- 156 Dunic, J. and Anderson, S. (2025) Assessing the quality of groundfish population indices derived  
from the Small-mesh Multi-species Bottom Trawl Survey. Technical Report Can. Tech. Rep. Fish.  
158 Aquat. Sci. nnn.
- IPHC (2024) *IPHC Fishery-Independent Setline Survey Sampling Manual (2024)*. URL <https://www.iphc.int/research/design-and-implementation/>.  
160
- Krishka, B.A., Starr, P.J. and Choromanski, E.M. (2005) Longspine thornyhead random strati-  
162 fied trawl survey off the west coast of Vancouver Island, September 4-21, 2003. *Can. Tech.*  
*Rep. Fish. Aquat. Sci.* **2577**, vi + 93 p. URL [https://publications.gc.ca/site/eng/422422/](https://publications.gc.ca/site/eng/422422/publication.html)  
164 [publication.html](https://publications.gc.ca/site/eng/422422/publication.html).
- Lacko, L., Acheson, S. and Holt, K. (2023) Summary of the annual 2021 Sablefish (*Anoplopoma*  
166 *fimbria*) trap survey, October 6 - November 21, 2021. *Can. Tech. Rep. Fish. Aquat. Sci.* **353**, vii  
+ 48 p.
- 168 McCullagh, P. and Nelder, J.A. (1989) *Generalized linear models*. Chapman & Hall, New York.
- Nottingham, M.K., Williams, D.C., Wyeth, M.R. and Olsen, N. (2017) Summary of the West Coast  
170 Vancouver Island synoptic bottom trawl survey, May 28 – June 21, 2014. *DFO Can. Manuscr.*  
*Rep. Fish. Aquat. Sci.* **2017/3140**, viii + 55 p.
- 172 Sinclair, A., Schnute, J., Haigh, R., Starr, P., Stanley, R., Fargo, J. and Workman, G. (2003)  
Feasibility of multispecies groundfish trawl surveys on the BC coast. *DFO Can. Sci. Adv. Sec.*  
174 *Res. Doc.* **2003/049**, i + 34 p.
- Sinclair, A. and Workman, G. (2002) A review of Pacific cod (*Gadus macrocephalus*) monitoring  
176 surveys in Hecate Strait, March–July 2002. *DFO Can. Sci. Adv. Sec. Res. Doc.* **2002/130**, 59 p.
- Starr, P.J., Krishka, B.A. and Choromanski, E.M. (2002) Trawl survey for thornyhead biomass esti-  
178 mation off the west coast of Vancouver Island, September 15 to October 2, 2001. *Can. Tech.*  
*Rep. Fish. Aquat. Sci.* **2421**, 60 p. URL [https://publications.gc.ca/site/eng/422422/](https://publications.gc.ca/site/eng/422422/publication.html)  
180 [publication.html](https://publications.gc.ca/site/eng/422422/publication.html).

- Williams, D.C., Nottingham, M.K., Olsen, N. and Wyeth, M.R. (2018a) Summary of the Queen  
182 Charlotte Sound synoptic bottom trawl survey, July 6 – August 8, 2015. *DFO Can. Manuscr.  
Rep. Fish. Aquat. Sci.* **3136**, viii + 64 p.
- 184 Williams, D.C., Nottingham, M.K., Olsen, N. and Wyeth, M.R. (2018b) Summary of the West Coast  
Haida Gwaii synoptic bottom trawl survey, August 25 – October 2, 2014. *DFO Can. Manuscr.  
186 Rep. Fish. Aquat. Sci.* **2018/3134**, viii + 42 p.
- Wyeth, M.R., Olsen, N., Nottingham, M.K. and Williams, D.C. (2018) Summary of the Hecate  
188 Strait synoptic bottom trawl survey, May 26 – June 22, 2015. *DFO Can. Manuscr. Rep. Fish.  
Aquat. Sci.* **2018/3126**, viii + 55 p.

190 **B Supporting tables and figures**

Table S1: Species included and their biological parameters. The estimated length-weight parameters, a and b, were estimated separately for males and females with fork lengths (or total lengths for chondrichthyans except for Spotted Ratfish which are measured to the back of second dorsal fin) measured in cm and weights in grams and using a Student-t distribution with degrees of freedom set to 3 to be robust to outliers ( $\log(W_i) \sim \text{Student-t}(3, \log(a) + b \log(L_i), \sigma)$ ; Figure S5). The length at 50% maturity is derived from a logistic regressions fit to individual fish specimens categorized as mature vs. not mature with set as random effect as long as at least 20 sets were available (Equations 1-3; Figure S3).

Species		ln(a)		b		Maturity (cm)	
Common name	Scientific name	Male	Female	Male	Female	Male	Female
Arrowtooth Flounder	<i>Atheresthes stomias</i>	-4.65	-4.86	2.97	3.05	31.9	38.4
Big Skate	<i>Beringraja binoculata</i>	-4.63	-4.71	2.94	2.97	102.9	113.1
Bocaccio	<i>Sebastes paucispinis</i>	-5.00	-4.88	3.14	3.11	40.7	45.0
Canary Rockfish	<i>Sebastes pinniger</i>	-4.08	-3.97	3.00	2.97	38.8	41.2
Darkblotched Rockfish	<i>Sebastes crameri</i>	-4.23	-4.11	3.07	3.04	31.6	34.6
Dover Sole	<i>Microstomus pacificus</i>	-5.40	-5.26	3.22	3.17	23.1	33.4
English Sole	<i>Parophrys vetulus</i>	-4.61	-4.88	2.97	3.06	20.9	29.2
Flathead Sole	<i>Hippoglossoides elassodon</i>	-5.04	-5.18	3.10	3.14	22.5	27.8
Greenstriped Rockfish	<i>Sebastes elongatus</i>	-4.80	-5.17	3.15	3.27	25.4	24.2
Lingcod	<i>Ophiodon elongatus</i>	-6.00	-5.77	3.32	3.25	58.6	68.7
Longnose Skate	<i>Raja rhina</i>	-5.62	-5.63	3.11	3.11	85.0	102.0
Pacific Cod	<i>Gadus macrocephalus</i>	-4.87	-4.87	3.09	3.09	48.7	50.9
Pacific Hake	<i>Merluccius productus</i>	-4.79	-4.98	2.94	2.99	40.7	44.1
Pacific Ocean Perch	<i>Sebastes alutus</i>	-4.55	-4.49	3.09	3.07	31.1	32.4
Pacific Sanddab	<i>Citharichthys sordidus</i>	-5.10	-5.24	3.18	3.24	18.3	16.2
Pacific Spiny Dogfish	<i>Squalus suckleyi</i>	-5.60	-6.19	3.01	3.17	71.0	86.3
Petrale Sole	<i>Eopsetta jordani</i>	-4.99	-5.33	3.14	3.24	33.9	36.5
Quillback Rockfish	<i>Sebastes maliger</i>	-4.18	-4.23	3.08	3.09	30.0	28.9
Redbanded Rockfish	<i>Sebastes babcocki</i>	-4.21	-4.48	3.05	3.13	35.5	38.9
Redstripe Rockfish	<i>Sebastes proriger</i>	-4.32	-4.43	3.00	3.04	24.5	27.1
Rex Sole	<i>Glyptocephalus zachirus</i>	-5.59	-5.61	3.17	3.18	24.5	25.6
Rosethorn Rockfish	<i>Sebastes helvomaculatus</i>	-4.80	-4.77	3.17	3.17	24.7	22.9
Sablefish	<i>Anoplopoma fimbria</i>	-5.33	-5.33	3.18	3.18	50.1	56.5
Sharpchin Rockfish	<i>Sebastes zacentrus</i>	-4.56	-4.63	3.10	3.13	22.0	24.2
Shortraker Rockfish	<i>Sebastes borealis</i>	-4.63	-4.76	3.12	3.16	45.0	49.9
Shortspine Thornyhead	<i>Sebastolobus alascanus</i>	-4.76	-4.81	3.12	3.14	19.6	22.6
Silvergray Rockfish	<i>Sebastes brevispinis</i>	-4.05	-3.79	2.93	2.87	42.4	42.3
Slender Sole	<i>Lyopsetta exilis</i>	-5.20	-5.16	3.08	3.07	23.0	21.9
Southern Rock Sole	<i>Lepidopsetta bilineata</i>	-4.70	-4.97	3.09	3.17	26.5	30.0
Spotted Ratfish	<i>Hydrolagus colliei</i>	-4.37	-4.32	2.97	2.95	30.2	39.3
Walleye Pollock	<i>Gadus chalcogrammus</i>	-4.84	-4.70	3.01	2.97	38.1	40.2
Widow Rockfish	<i>Sebastes entomelas</i>	-4.50	-4.21	3.09	3.00	38.7	39.7
Yelloweye Rockfish	<i>Sebastes ruberrimus</i>	-4.16	-4.23	3.05	3.07	46.5	41.5
Yellowmouth Rockfish	<i>Sebastes reedi</i>	-4.85	-4.67	3.20	3.14	36.1	36.8
Yellowtail Rockfish	<i>Sebastes flavidus</i>	-4.26	-4.21	3.03	3.02	36.9	39.6

Table S2: List of survey abbreviations included as factor levels in the total biomass density model for each species (see ‘Fishery-independent survey data’ section). Some subset of these were included for each maturity class when that maturity class was detected, or deemed to have been (see ‘Decision rules for splitting total catches from unsampled tows’ section) in at least 3 years and > 1% of tows overall for that survey. The MSSM survey was split into two factors: MSSM<=05 for years before gear change in 2006 and MSSM>05 for years after.

Species	Surveys included in total biomass density model
Arrowtooth Flounder	SYN, MSSM<=05, MSSM>05, MSA, HS PCOD, THORNYHEAD, HAKE
Big Skate	SYN, MSSM<=05, MSSM>05, MSA
Bocaccio	SYN, MSSM<=05, MSSM>05, MSA, HS PCOD
Canary Rockfish	SYN, MSSM<=05, MSSM>05, MSA, HS PCOD
Darkblotched Rockfish	SYN, MSSM<=05, MSSM>05, HS PCOD
Dover Sole	SYN, MSSM<=05, MSSM>05, MSA, HS PCOD, THORNYHEAD
English Sole	SYN, MSA, MSSM<=05, MSSM>05
Flathead Sole	SYN, MSSM<=05, MSSM>05, MSA, HS PCOD
Greenstriped Rockfish	SYN, HS PCOD, MSSM<=05, MSSM>05
Lingcod	SYN, MSA, MSSM<=05, MSSM>05
Longnose Skate	SYN, MSSM<=05, MSSM>05, MSA, HS PCOD, THORNYHEAD
Pacific Cod	SYN, MSSM<=05, MSSM>05, MSA, HS PCOD
Pacific Hake	SYN, MSSM<=05, MSSM>05, HS PCOD, THORNYHEAD, HAKE
Pacific Ocean Perch	SYN, MSSM<=05, MSSM>05, MSA, HAKE
Pacific Sanddab	SYN, MSSM<=05, MSSM>05, MSA, HS PCOD
Pacific Spiny Dogfish	SYN, MSSM<=05, MSSM>05, MSA, HS PCOD, HAKE
Petrable Sole	SYN, MSSM<=05, MSSM>05, MSA, HS PCOD
Quillback Rockfish	SYN, MSA, HS PCOD
Redbanded Rockfish	SYN, MSSM<=05, MSSM>05, HS PCOD
Redstripe Rockfish	SYN, MSSM<=05, MSSM>05, HS PCOD, HAKE
Rex Sole	SYN, MSSM<=05, MSSM>05, MSA, HS PCOD, THORNYHEAD
Rosethorn Rockfish	SYN
Sablefish	SYN, MSSM<=05, MSSM>05, MSA, OTHER, HAKE
Sharpchin Rockfish	SYN, MSSM<=05, MSSM>05
Shortraker Rockfish	SYN, THORNYHEAD
Shortspine	SYN, MSSM<=05, MSSM>05, THORNYHEAD
Thornyhead	
Silvergray Rockfish	SYN, MSSM<=05, MSSM>05, MSA, HS PCOD, HAKE
Slender Sole	SYN, MSSM<=05, MSSM>05, MSA, HS PCOD
Southern Rock Sole	SYN, MSSM<=05, MSSM>05, MSA, HS PCOD
Spotted Ratfish	SYN, MSSM<=05, MSSM>05, MSA, HS PCOD
Walleye Pollock	SYN, MSSM<=05, MSSM>05, MSA, HS PCOD, HAKE
Widow Rockfish	SYN, MSSM<=05, MSSM>05, HAKE
Yelloweye Rockfish	SYN, MSSM<=05
Yellowmouth Rockfish	SYN, MSSM<=05, MSSM>05, HAKE
Yellowtail Rockfish	SYN, MSSM<=05, MSSM>05, MSA, HS PCOD, HAKE

Table S3: Counts of fish used in body condition analyses. All included specimens had length and weight measurements within 2 SD of a heavy-tailed distribution for the species. Unknown sex individuals were included only when smaller than the length at 50% maturity. Only specimens from survey types with more than 30 specimens collected from 2002 and June 2024 belonging to each maturity class of each species were included. Survey types included were bottom trawl surveys with mesh sizes targeting commercial groundfish species (TRAWL: includes modern synoptic and 3 historical surveys), small-mesh bottom trawl surveys targeting shrimp (MSSM), longline surveys targeting rockfish (HBLL), a longline survey for Pacific Halibut (IPHC FISS), and an integrated acoustic-trawl survey for Pacific Hake (HAKE). Table continues on next page.

Species	Survey	Immatures	Mature females	Mature males	Total
Arrowtooth Flounder	TRAWL	20826	25012	16408	62246
	MSSM	3094	1429	929	5452
	HAKE	35	113	48	196
Big Skate	TRAWL	673	76	162	911
	MSSM	552	0	56	608
Bocaccio	TRAWL	1360	1659	2430	5449
	MSSM	184	79	189	452
	IPHC FISS	0	41	56	97
	HBLL	0	31	42	73
	HAKE	52	0	0	52
Canary Rockfish	TRAWL	2866	2843	4376	10085
	HBLL	560	545	534	1639
	IPHC FISS	35	177	102	314
	MSSM	31	81	145	257
	HAKE	0	37	60	97
Darkblotched Rockfish	TRAWL	2255	838	1211	4304
	MSSM	747	0	0	747
Dover Sole	TRAWL	5579	15353	28470	49402
	MSSM	3191	1954	2364	7509
	HAKE	0	0	68	68
English Sole	TRAWL	7911	14571	11400	33882
	MSSM	841	1487	1154	3482
Flathead Sole	TRAWL	3249	7230	7512	17991
	MSSM	448	296	456	1200
Greenstriped Rockfish	TRAWL	2764	4735	3769	11268
	HBLL	0	236	37	273
	MSSM	128	39	51	218
Lingcod	TRAWL	5254	2312	1310	8876
	HBLL	506	1661	999	3166
	MSSM	1304	1011	330	2645
	IPHC FISS	0	113	0	113
Longnose Skate	MSSM	4544	47	229	4820
	TRAWL	1911	332	593	2836
Pacific Cod	TRAWL	24577	4987	4631	34195
	MSSM	3600	1604	1287	6491
Pacific Hake	TRAWL	1801	10326	4659	16786
	HAKE	1689	5298	4608	11595
	MSSM	821	90	52	963
Pacific Ocean Perch	TRAWL	15912	21156	24628	61696
	MSSM	526	32	113	671
	HAKE	0	280	167	447
Pacific Sanddab	TRAWL	2395	7207	4380	13982
	MSSM	0	110	95	205

Species	Survey	Immatures	Mature females	Mature males	Total
Pacific Spiny Dogfish	TRAWL	6324	338	2379	9041
	MSSM	779	59	306	1144
	HAKE	57	0	0	57
Petrale Sole	TRAWL	7482	7469	6079	21030
	MSSM	1432	2668	702	4802
Quillback Rockfish	HBLL	590	8919	10554	20063
	TRAWL	1548	1778	1660	4986
	IPHC FISS	0	924	895	1819
Redbanded Rockfish	TRAWL	7715	4805	7034	19554
	IPHC FISS	73	4805	3352	8230
	HBLL	303	2138	1842	4283
Redstripe Rockfish	TRAWL	3159	8256	8000	19415
	HAKE	48	515	285	848
	MSSM	69	0	0	69
Rex Sole	TRAWL	6669	23496	31587	61752
	MSSM	4089	2722	3438	10249
	HAKE	0	0	37	37
Rosethorn Rockfish	TRAWL	3022	3494	3288	9804
	HBLL	0	163	164	327
Sablefish	TRAWL	16327	2970	8590	27887
	MSSM	4214	0	67	4281
	HAKE	89	0	0	89
Sharpchin Rockfish	TRAWL	4691	8470	6947	20108
	MSSM	42	0	0	42
Shortraker Rockfish	TRAWL	0	1052	930	1982
	IPHC FISS	0	134	177	311
Shortspine Thornyhead	TRAWL	5746	11758	13802	31306
Silvergray Rockfish	TRAWL	1113	9064	14527	24704
	HBLL	86	263	256	605
	IPHC FISS	0	219	336	555
	HAKE	0	76	68	144
	MSSM	0	0	31	31
Slender Sole	TRAWL	5423	3449	1005	9877
	MSSM	511	147	0	658
Southern Rock Sole	TRAWL	10531	7744	2565	20840
	MSSM	40	0	0	40
Spotted Ratfish	TRAWL	13720	1689	5958	21367
	MSSM	70	35	110	215
Walleye Pollock	TRAWL	13363	5091	1946	20400
	MSSM	7501	692	282	8475
	HAKE	404	698	650	1752
Widow Rockfish	TRAWL	719	806	942	2467
	HAKE	135	107	36	278
Yelloweye Rockfish	HBLL	2838	13108	9912	25858
	IPHC FISS	296	4094	5015	9405
	TRAWL	423	755	604	1782
Yellowmouth Rockfish	TRAWL	3149	3327	3265	9741
	HAKE	58	139	57	254
	HBLL	0	0	51	51
	IPHC FISS	0	0	31	31
Yellowtail Rockfish	TRAWL	1795	3335	5497	10627
	HAKE	0	276	380	656
	MSSM	0	138	238	376
	HBLL	0	32	40	72

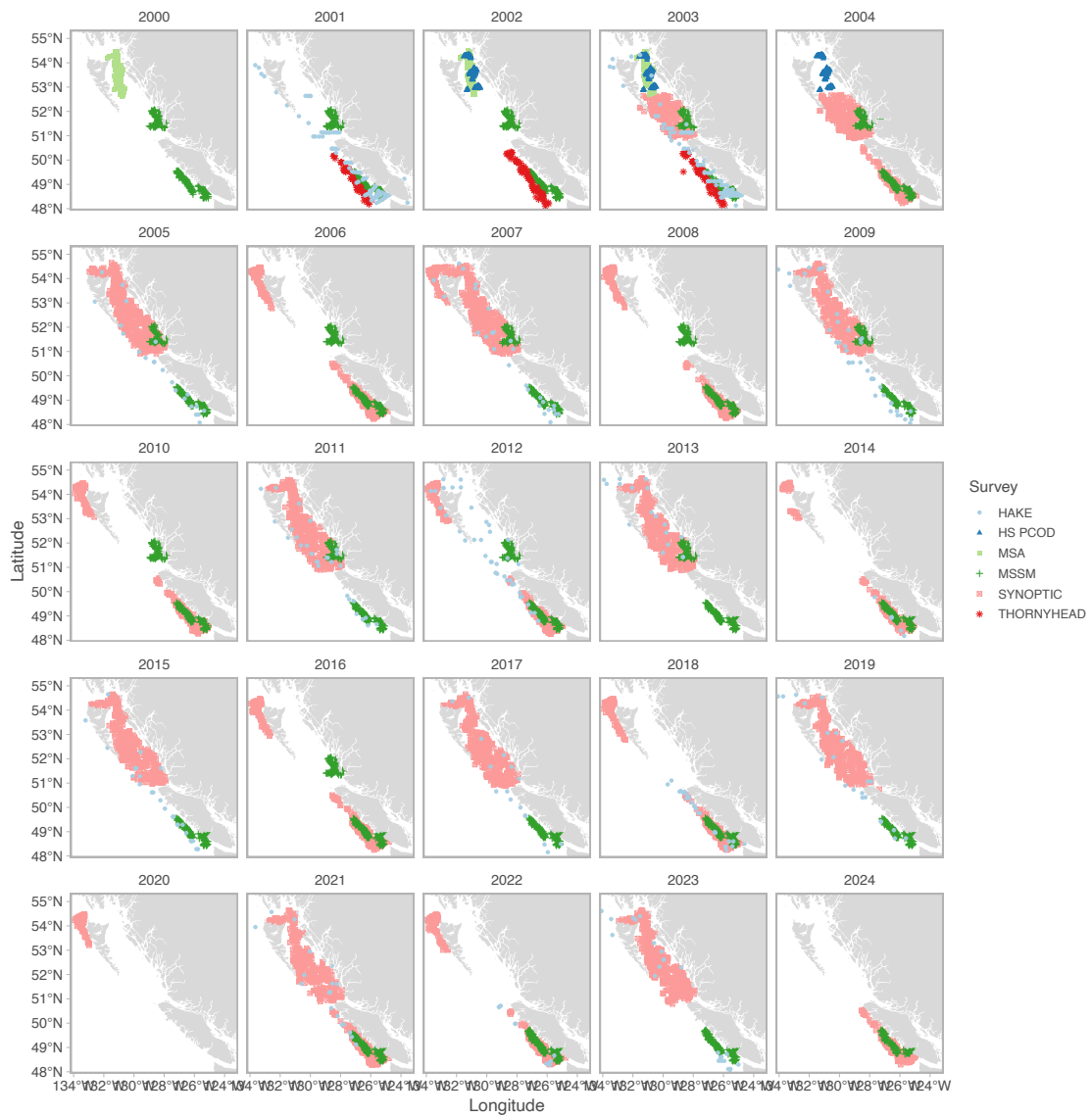


Figure S1: Spatial and temporal distribution of fisher-independent surveys using trawl gear in Canadian Pacific waters. All are bottom trawl except HAKE, which targets schools of Pacific Hake in the midwater. Grey areas represent land, mostly British Columbia, Canada.

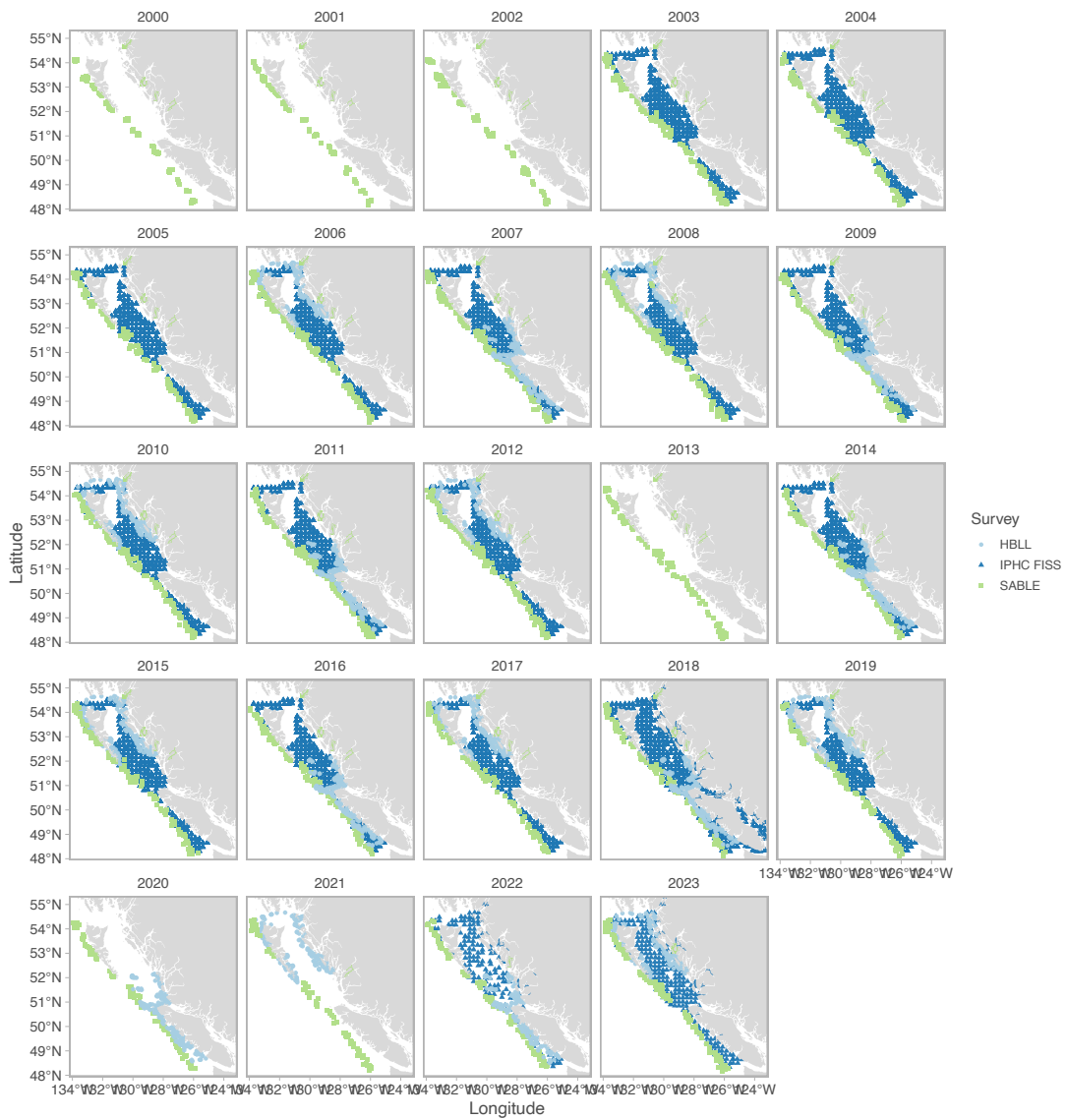


Figure S2: Spatial and temporal distribution of fisher-independent surveys using longline hook (HLL and IPHC FISS) or trap (SABLE) gear in Canadian Pacific waters.

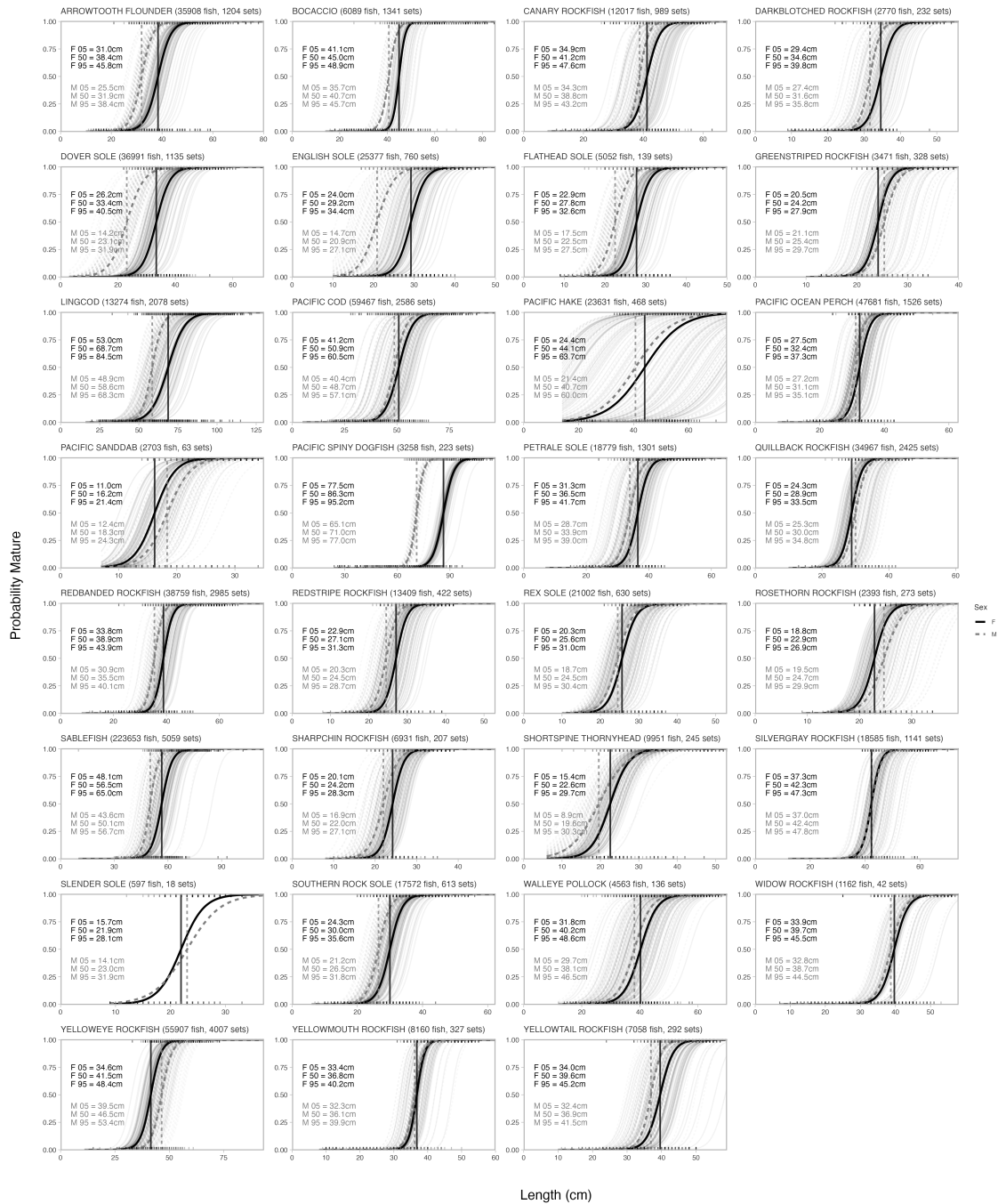


Figure S3: Plots of maturity ogives for males and females on average in bold with set-level random effect estimates in background. Black solid lines represent females and grey dashed lines for males. Estimated length at 5, 50, 95% mature for each sex and overall sample sizes are indicated on each panel.

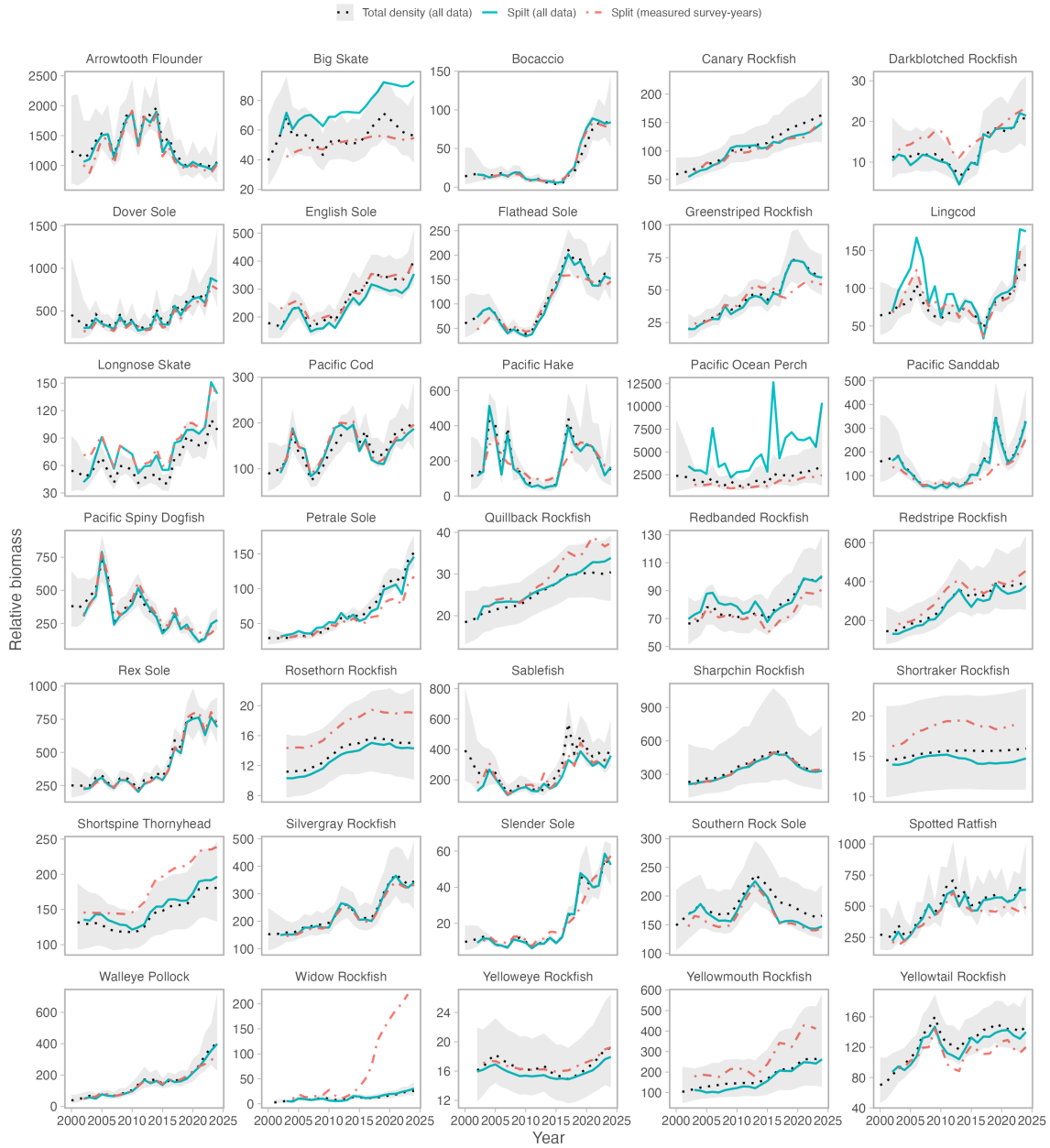


Figure S4: Comparison of total biomass index modelled from total catches from all surveys with positive catches in  $\geq 3$  years and on  $> 1\%$  of tows (dotted black line) with sums of maturity class specific indices based on two sets of data. Solid blue line using all the same data points as the dotted line, but relies on averages from other years or surveys for splitting catches in survey-year combinations without morphological data. Dashed red line uses only survey-years with morphological data from  $\geq 18$  fish and  $\geq 6$  tows.

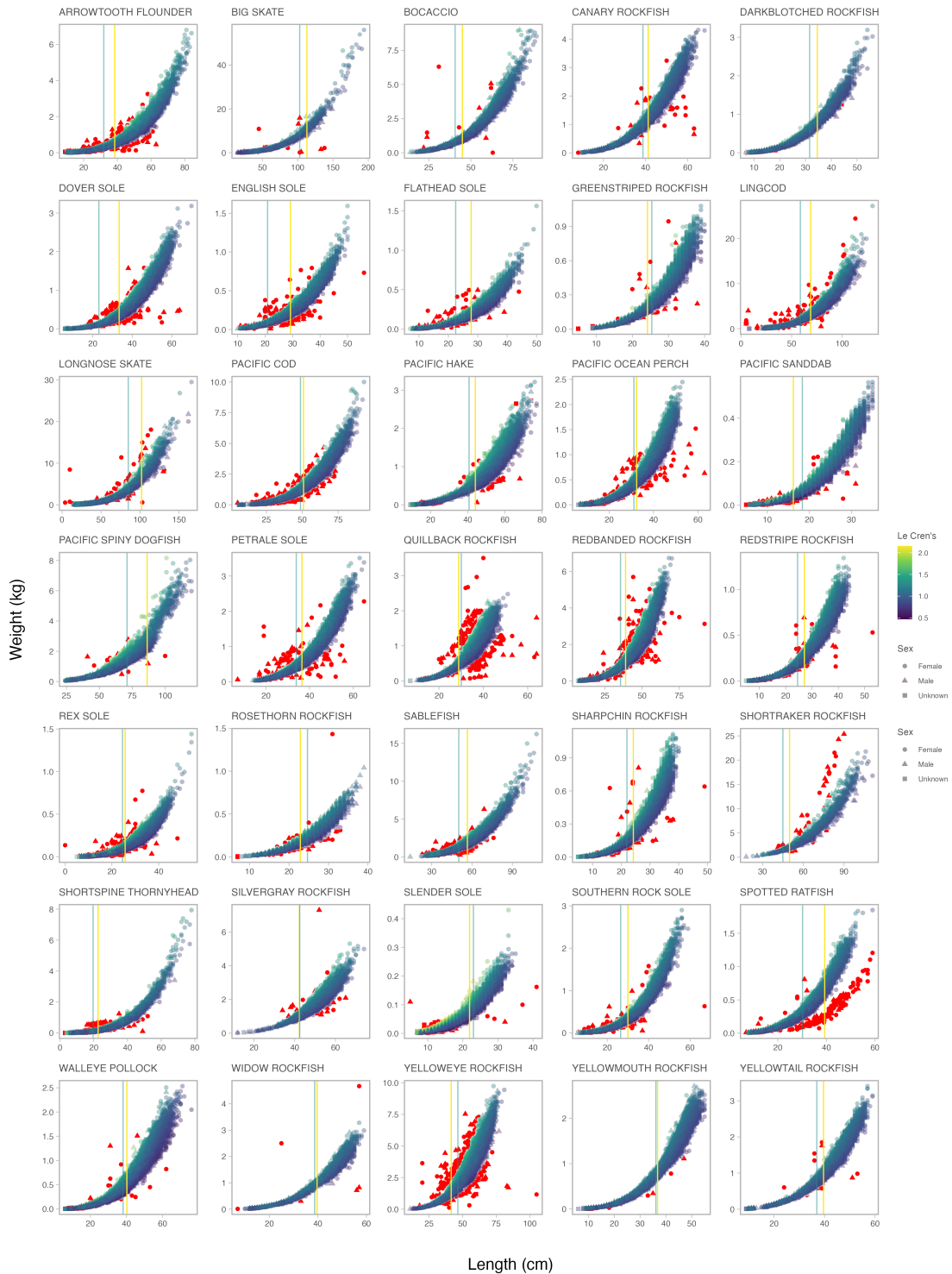


Figure S5: Le Cren's condition factors plotted on the length-weight relationships for all all species. Red points are outliers based on length-weight residuals being  $> 2x$  the scale parameter estimated for the Student t distribution ( $df = 3$ ) for each sex separately. Shape indicates the sex of individual fish. Vertical lines indicate lengths of 50% maturity (purple = males, yellow = female).

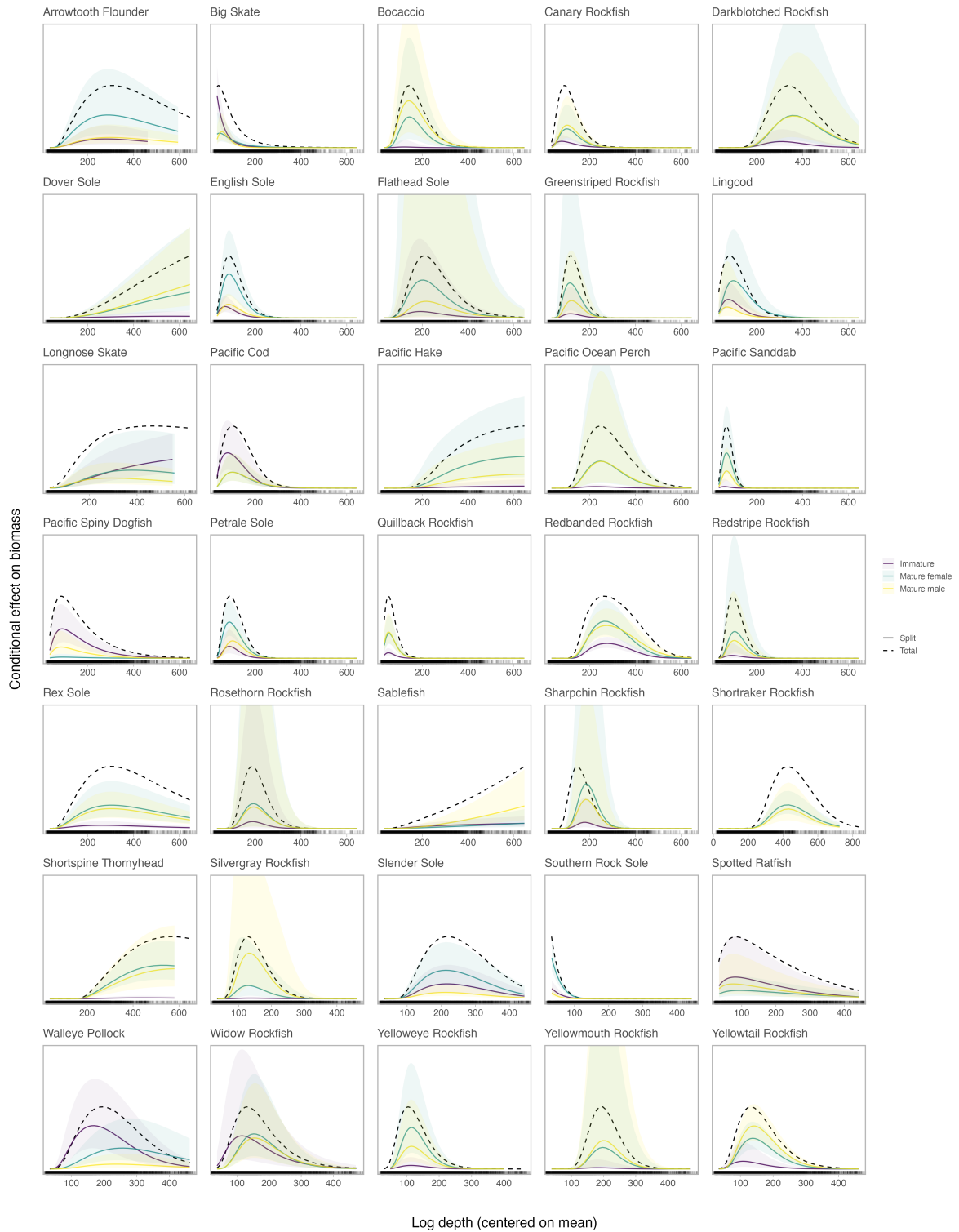


Figure S6: Effects of depth on biomass density for overall abundance (dashed line) and for each sex and maturity class (solid coloured lines). Shading represents 95% CI for class-specific relationships.

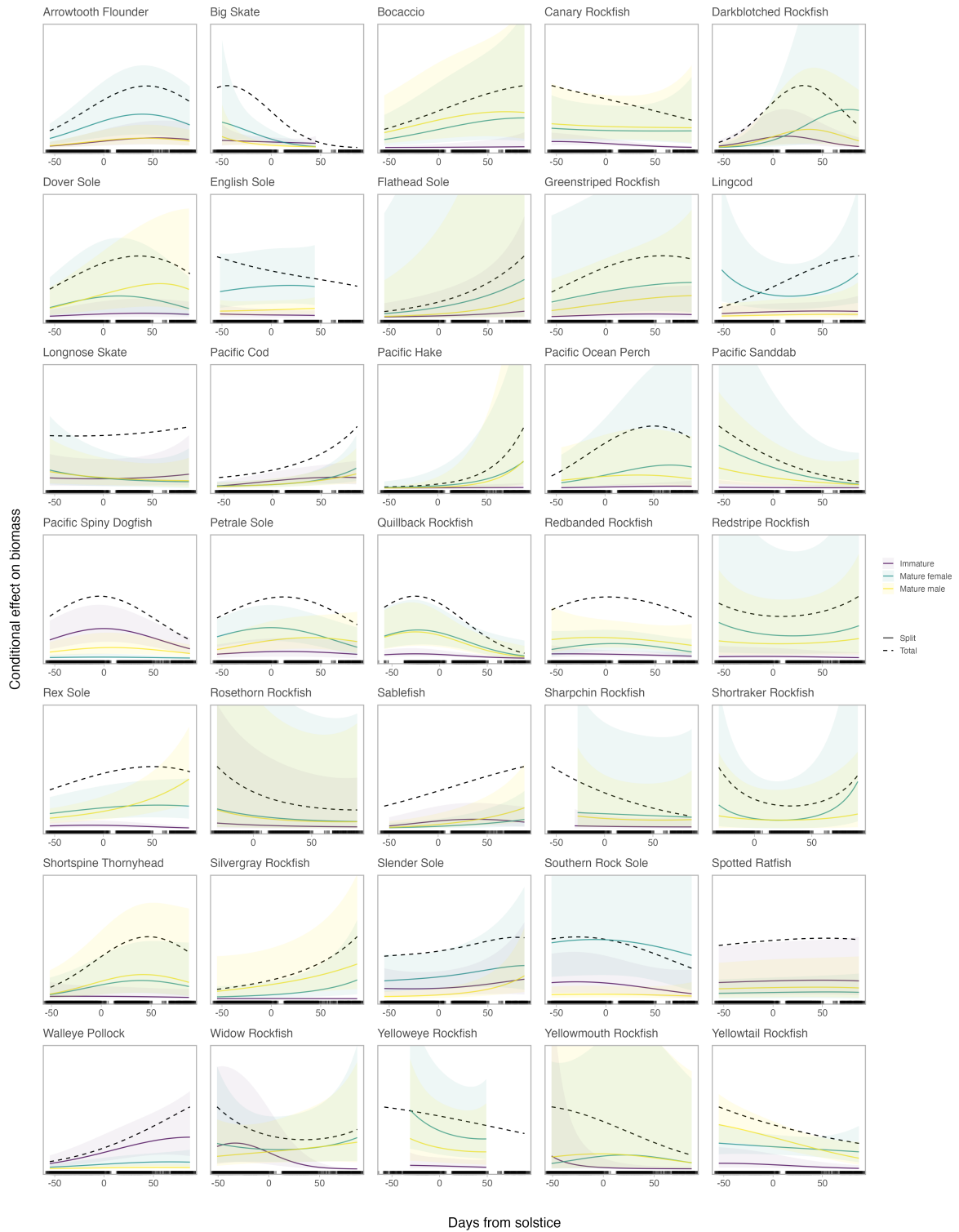


Figure S7: Effects of date, in days from solstice, on biomass density for overall abundance (dashed line) and for each sex and maturity class (solid coloured lines). Shading represents 95% CI for class-specific relationships.

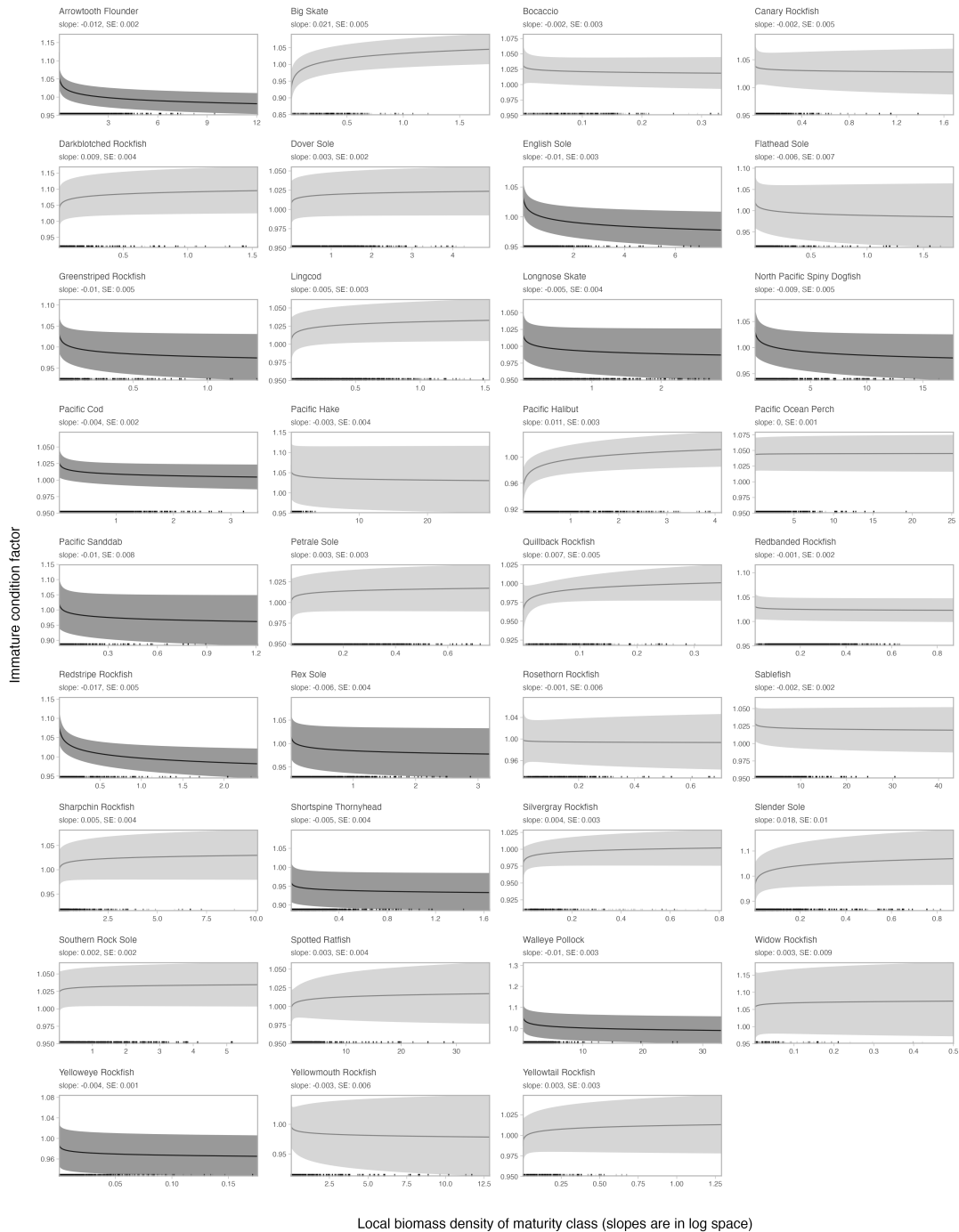
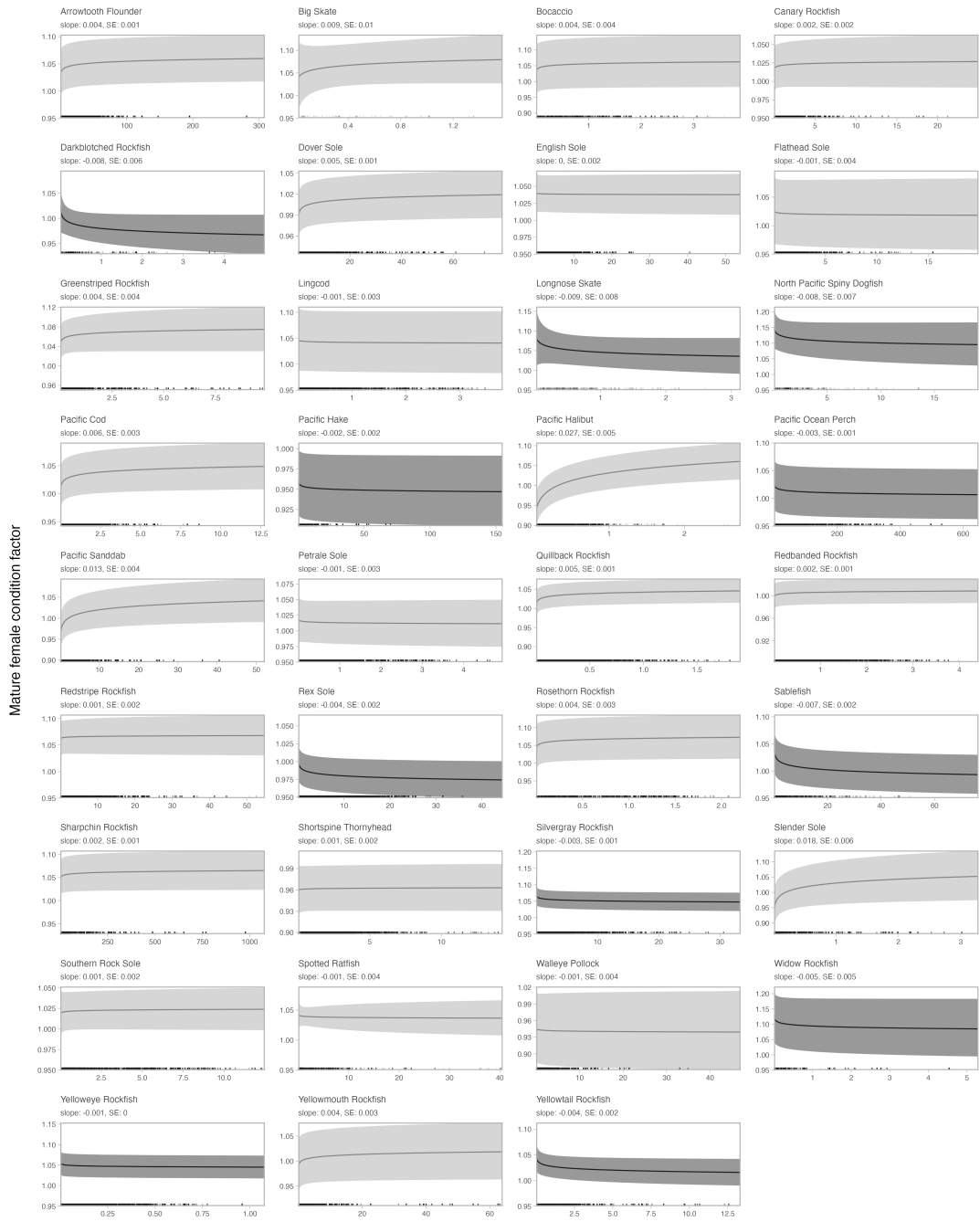


Figure S8: Effect of local immature density on immature condition factors. Darker shading indicates when the effect of density is negative by more than the SE on the estimate. We only account for density before investigating environmental correlations in these cases, because positive relationships are likely to be the result of individuals congregating where conditions are good, rather than competition.



Figure S9: Effect of local total biomass density on mature male condition factors. Shading as described in Figure S8.



Local biomass density of maturity class (slopes are in log space)

Figure S10: Effect of local total biomass density on mature female condition factors. Shading as described in Figure S10.

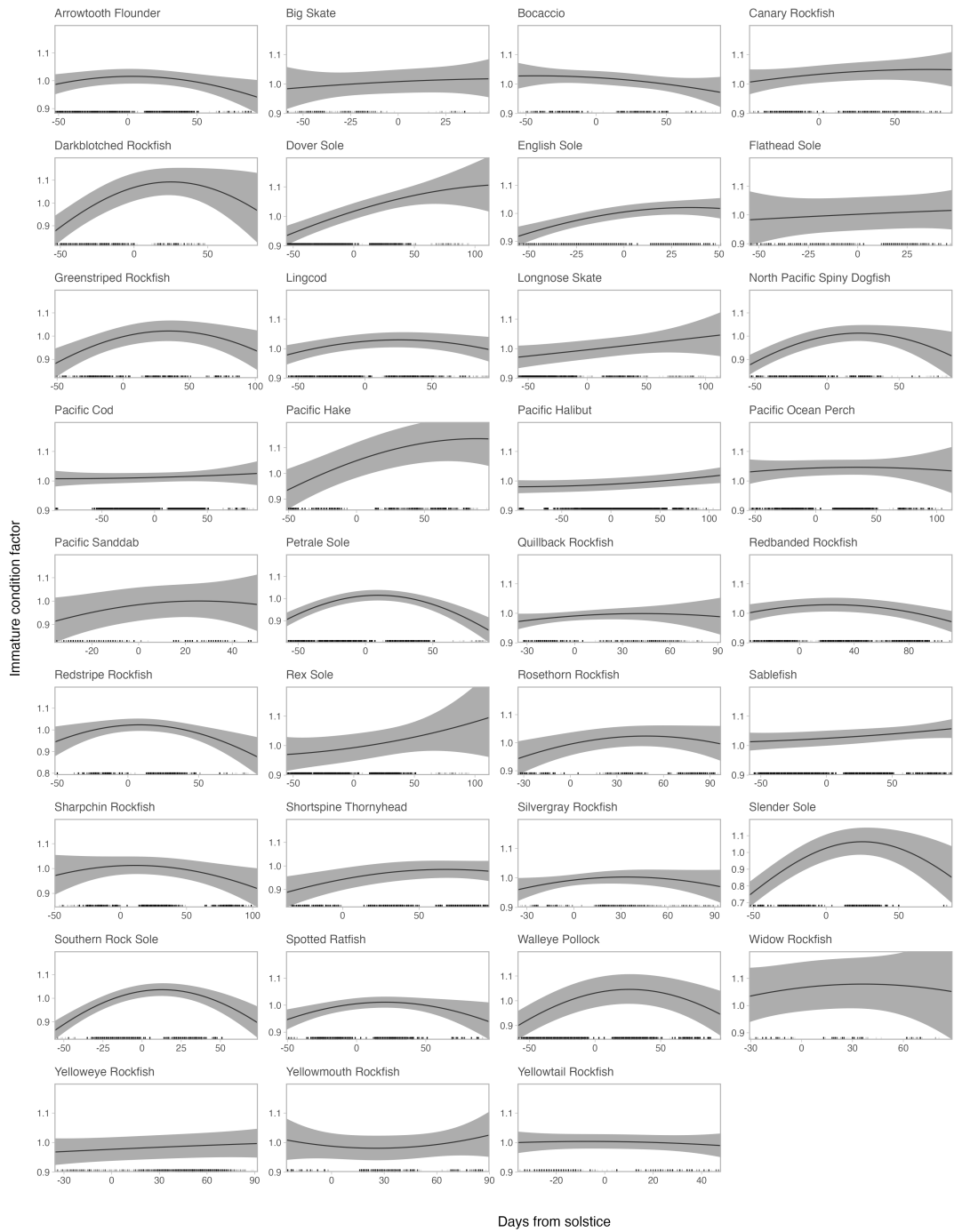


Figure S11: Effect of date, as days from summer solstice, on immature condition factors.

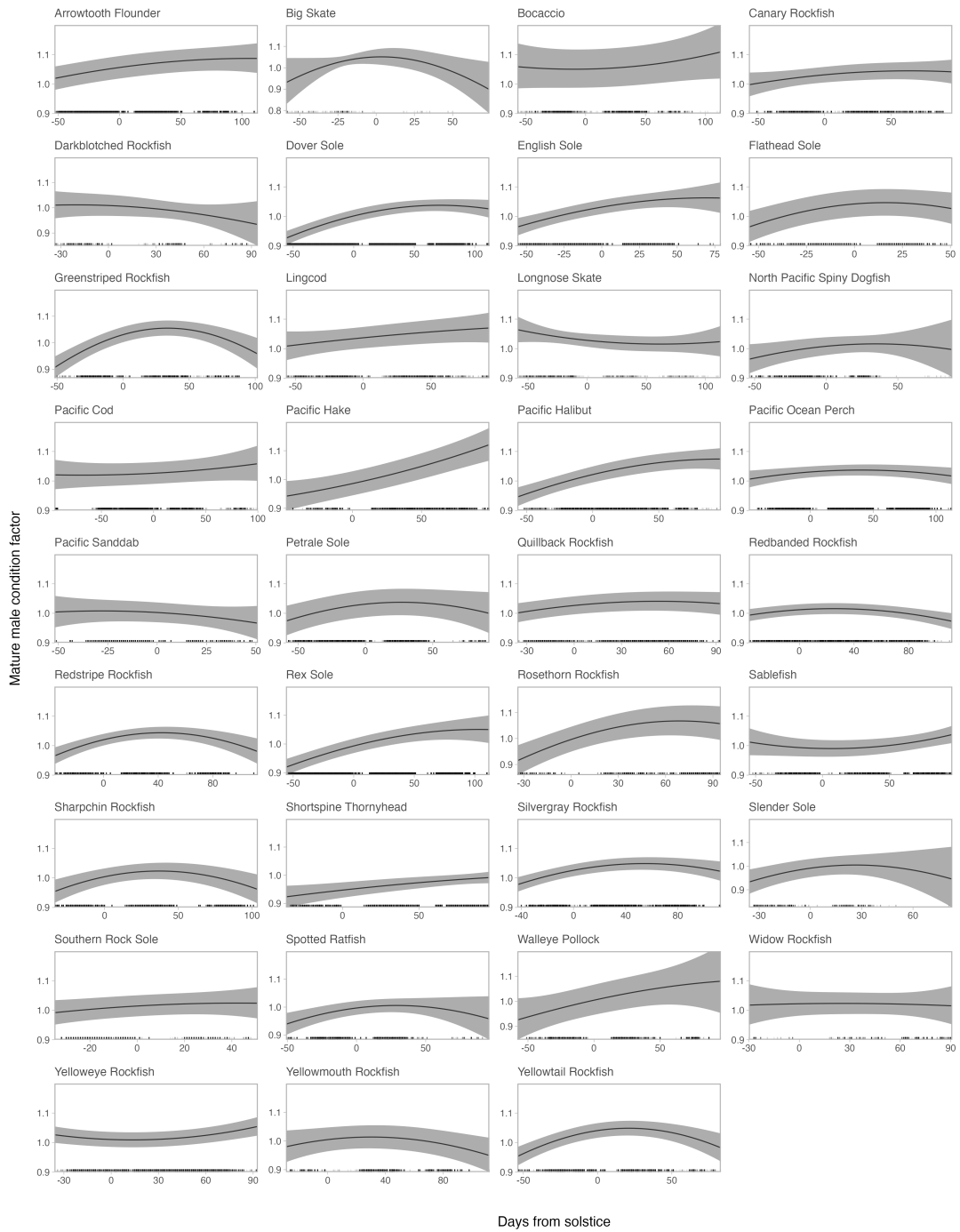


Figure S12: Effect of date, as days from summer solstice, on mature male condition factors.

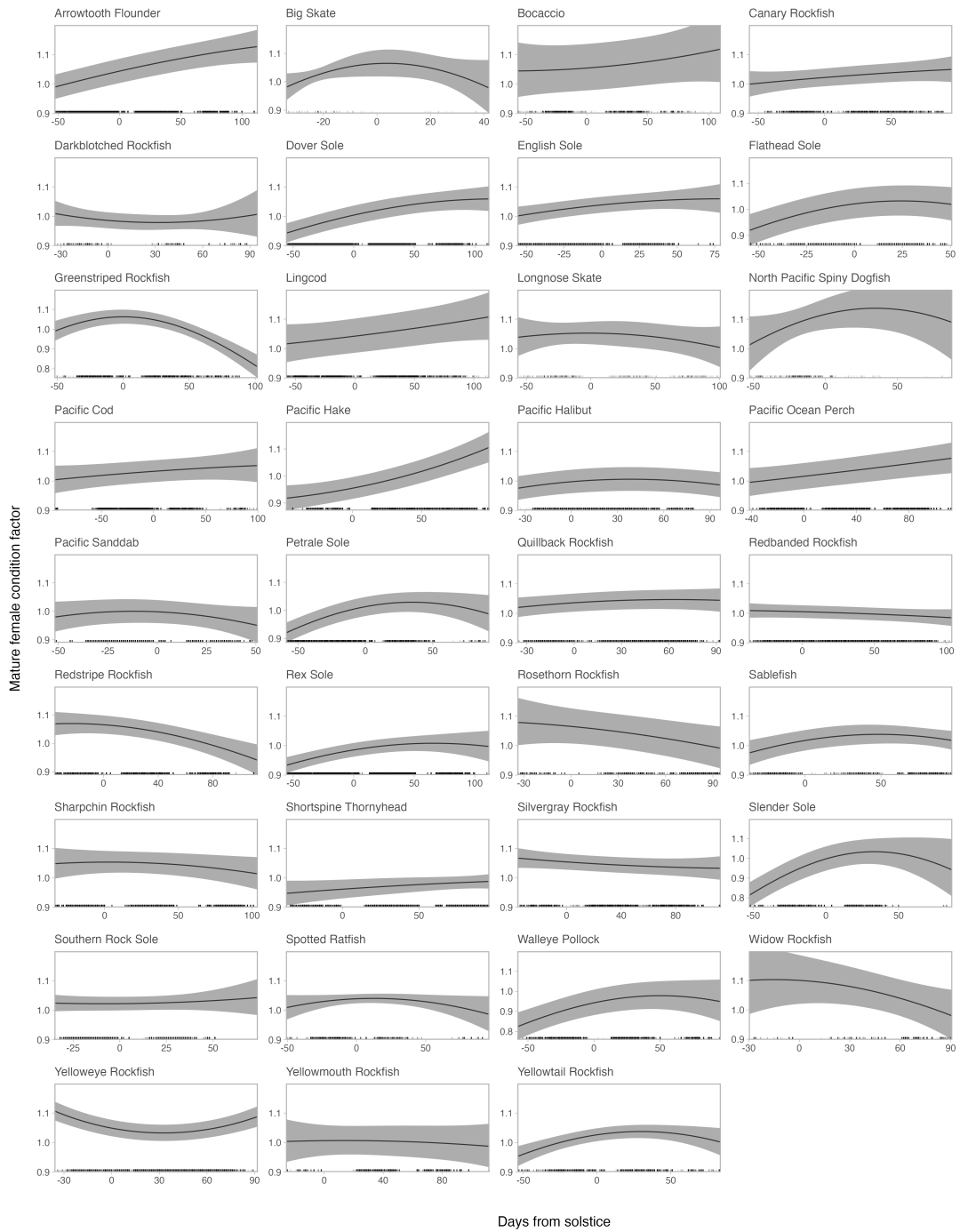


Figure S13: Effect of date, as days from summer solstice, on mature female condition factors.

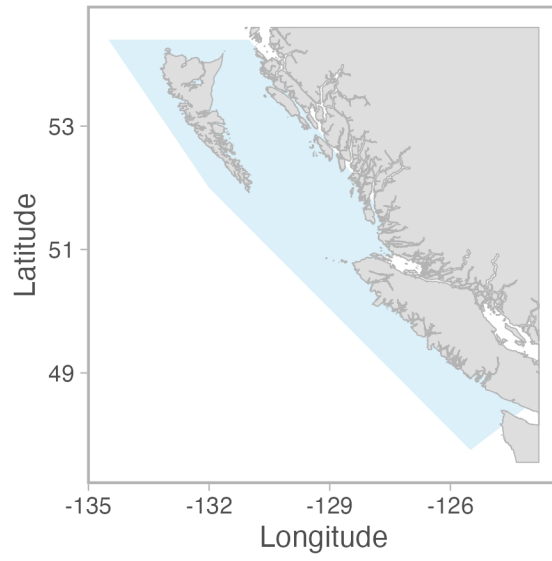


Figure S14: Extent of the Pacific Ocean for which spatially explicit environmental variables (e.g., SST and primary production) were aggregated for comparison against common trends in body condition.

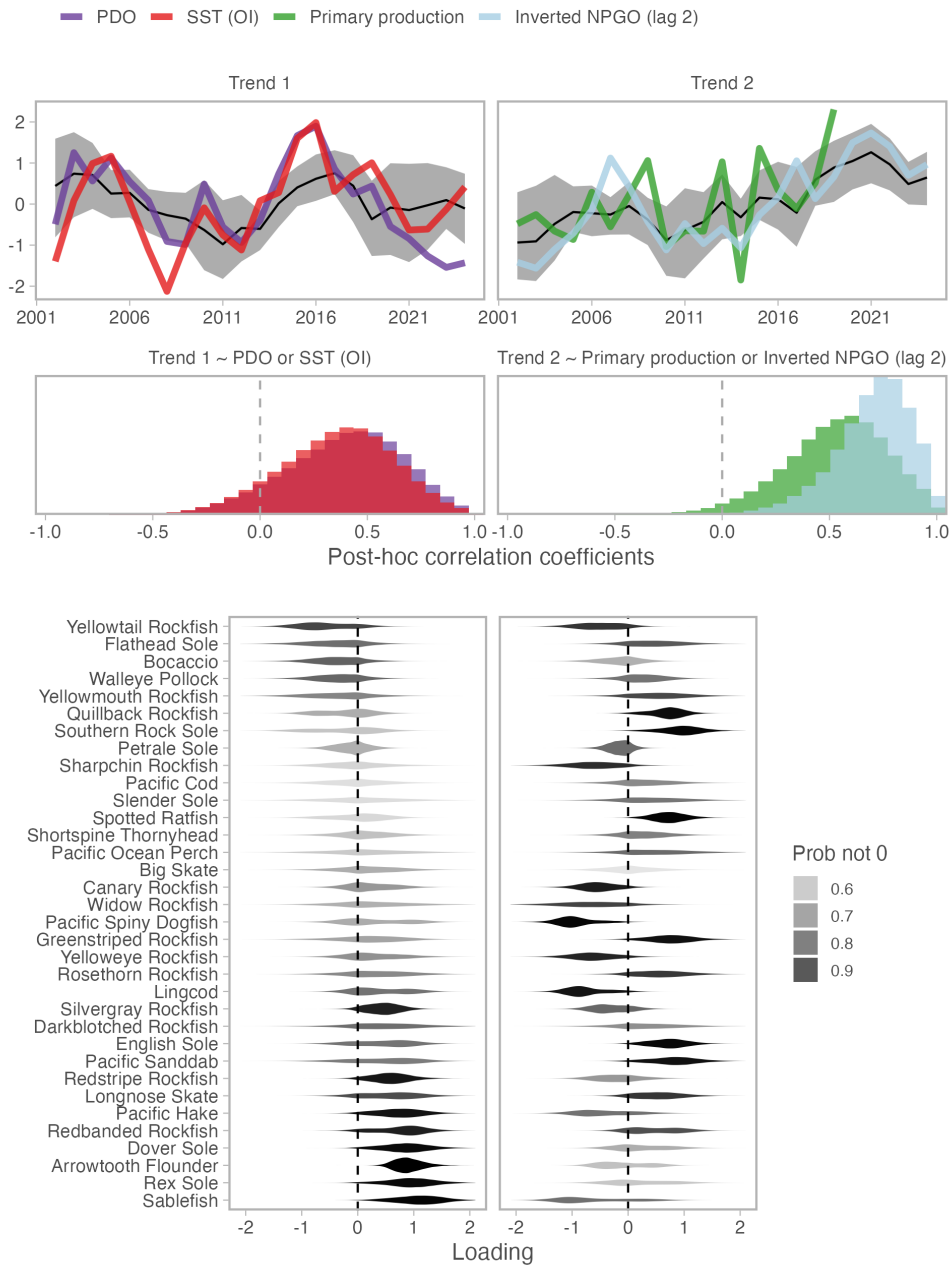


Figure S15: Common trends in density-agnostic immature body condition (top row) are most correlated with PDO (trend 1) and NPGO (trend 2) as indicated by histograms of post-hoc correlation coefficients (middle row). Shading on violin plots indicate how different from zero the posterior for each loading is (bottom plot). Species with a strong positive relationship with a given trend, and therefore any environmental variables also positively correlated with that trend, have dark violins on the right of the dashed lines; those with strong negative relationships have dark violins to the left of the dashed lines. Environmental variables negatively related to a trend will have an impact in the opposite direction of the loading for each species.

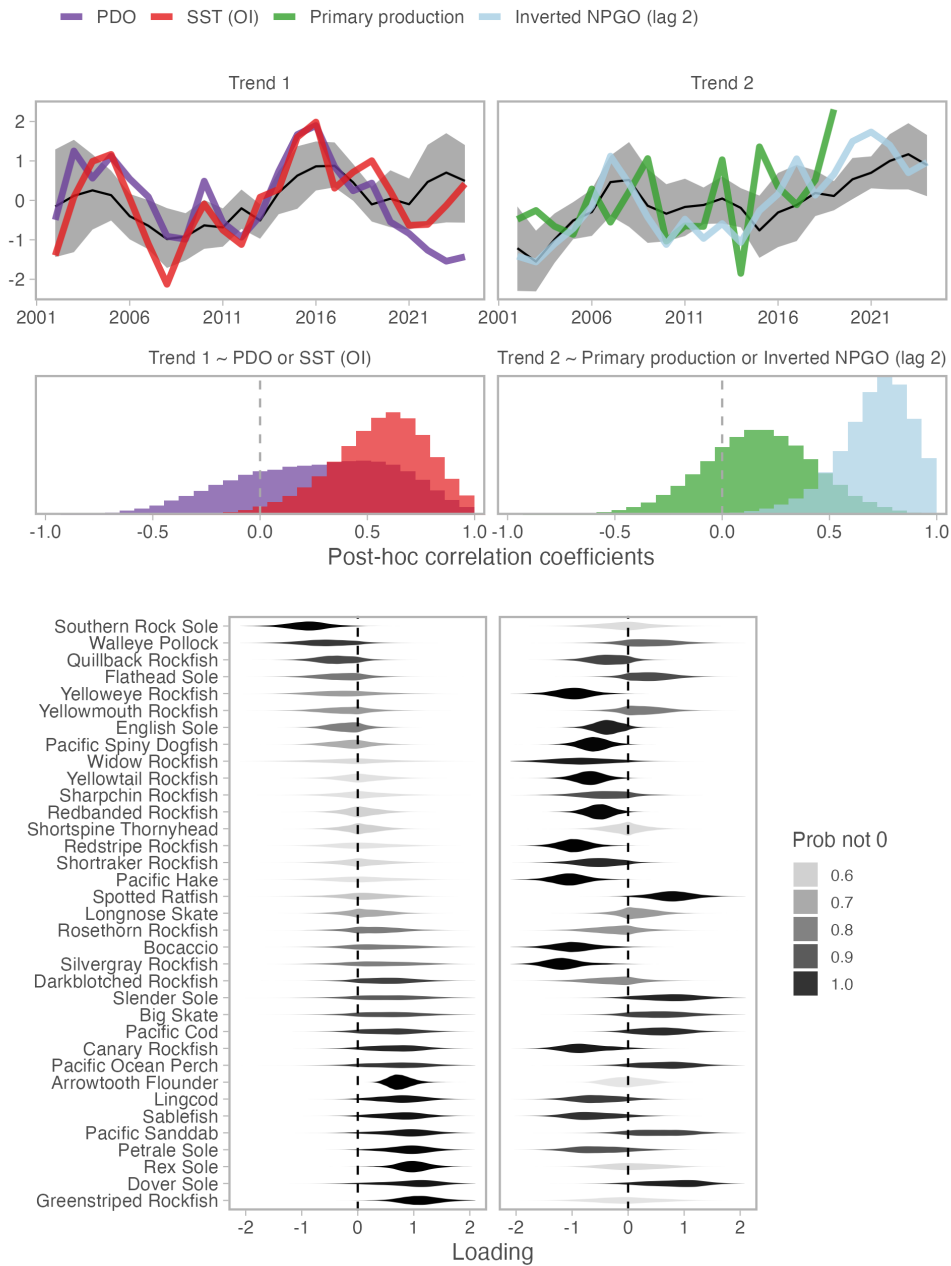


Figure S16: Common trends in density-agnostic mature male body condition (top row) are most correlated with SST (trend 1) and NPGO (trend 2) as indicated by histograms of post-hoc correlation coefficients (middle row). Shading on violin plots indicate how different from zero the posterior for each loading is (bottom plot). Species with a strong positive relationship with a given trend, and therefore any environmental variables also positively correlated with that trend, have dark violins on the right of the dashed lines; those with strong negative relationships have dark violins to the left of the dashed lines. Environmental variables negatively related to a trend will have an impact in the opposite direction of the loading for each species.

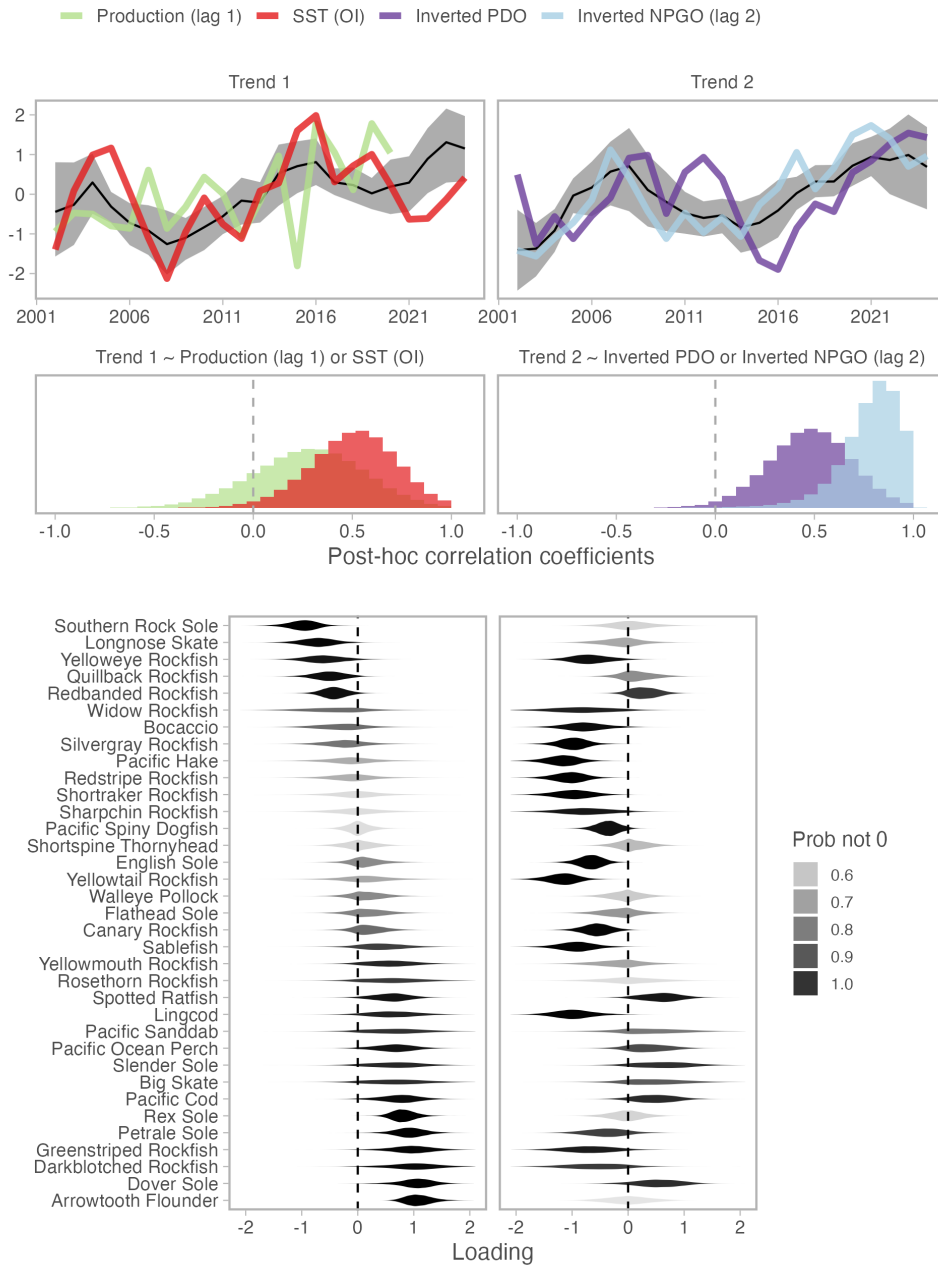


Figure S17: Common trends in density-agnostic mature female body condition (top row) are most correlated with SST (trend 1) and NPGO (trend 2) as indicated by histograms of post-hoc correlation coefficients (middle row). Shading on violin plots indicate how different from zero the posterior for each loading is (bottom plot). Species with a strong positive relationship with a given trend, and therefore any environmental variables also positively correlated with that trend, have dark violins on the right of the dashed lines; those with strong negative relationships have dark violins to the left of the dashed lines.

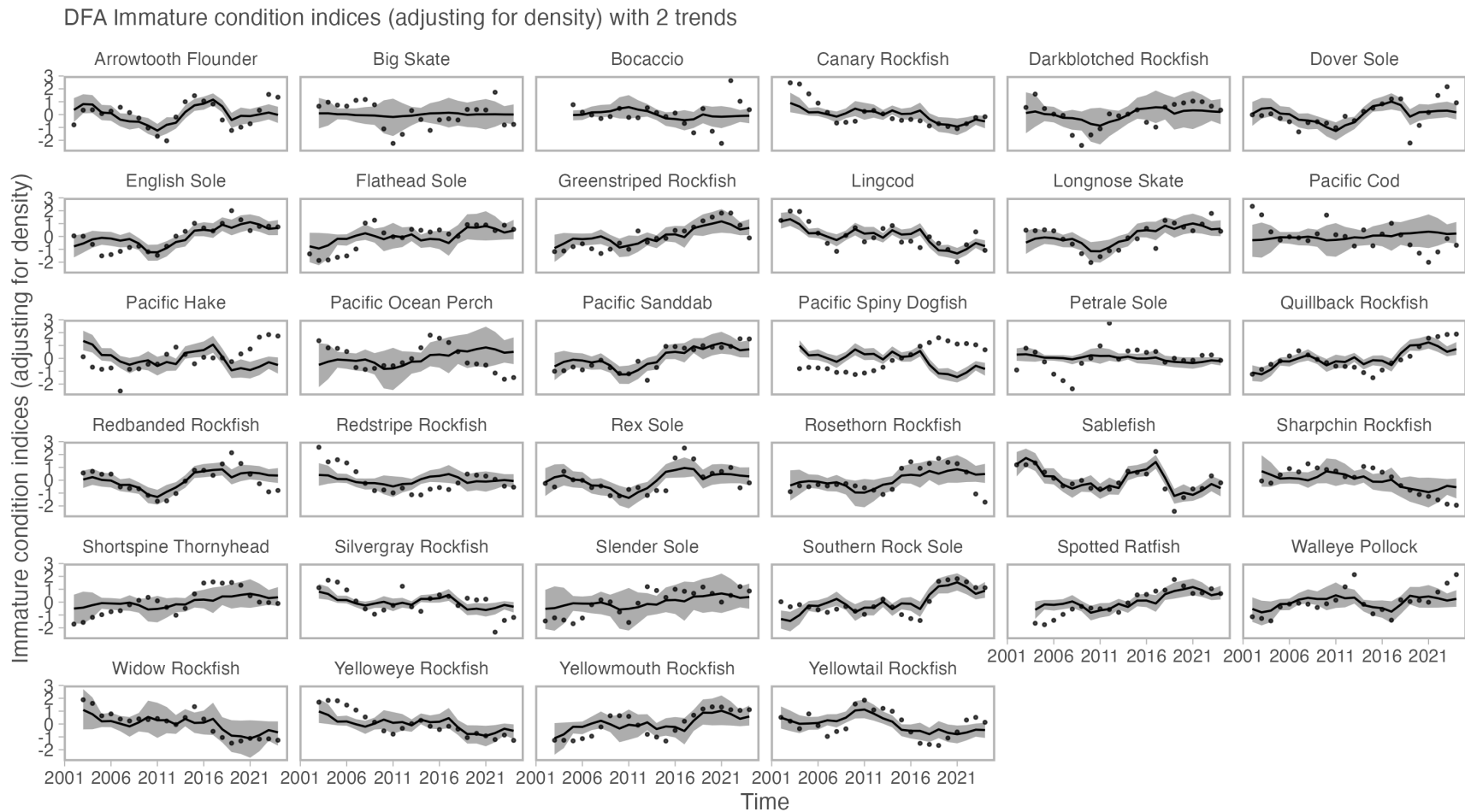


Figure S18: Fit of DFA-derived annual estimates of immature body condition for each species based on two common trends and species-specific loadings (black line and grey ribbon) and the spatiotemporal model-derived indices of average body condition adjusted for local biomass density (black dots).

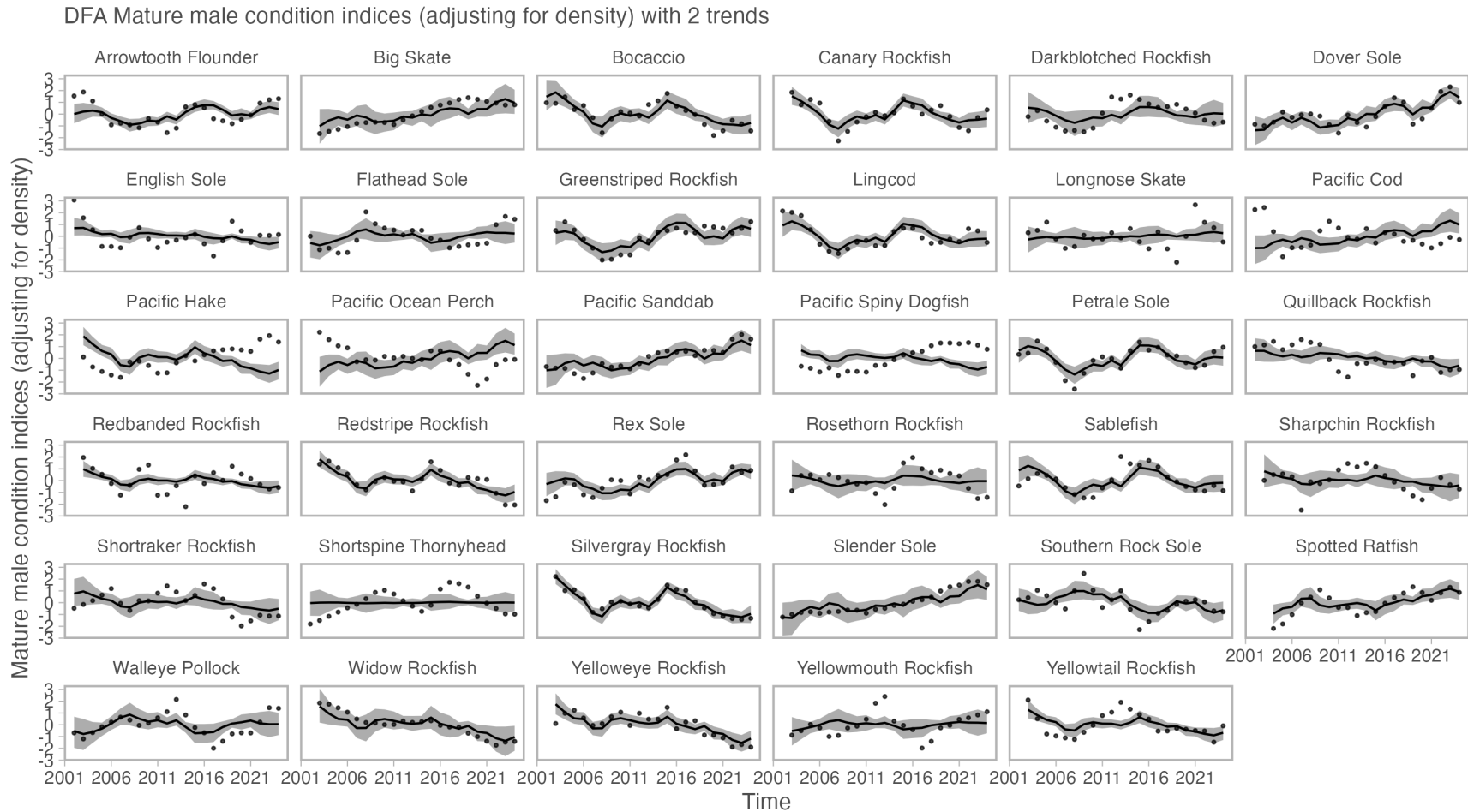


Figure S19: Fit of DFA-derived annual estimates of mature male body condition for each species based on two common trends and species-specific loadings (black line and grey ribbon) and the spatiotemporal model-derived indices of average body condition adjusted for local biomass density (black dots).

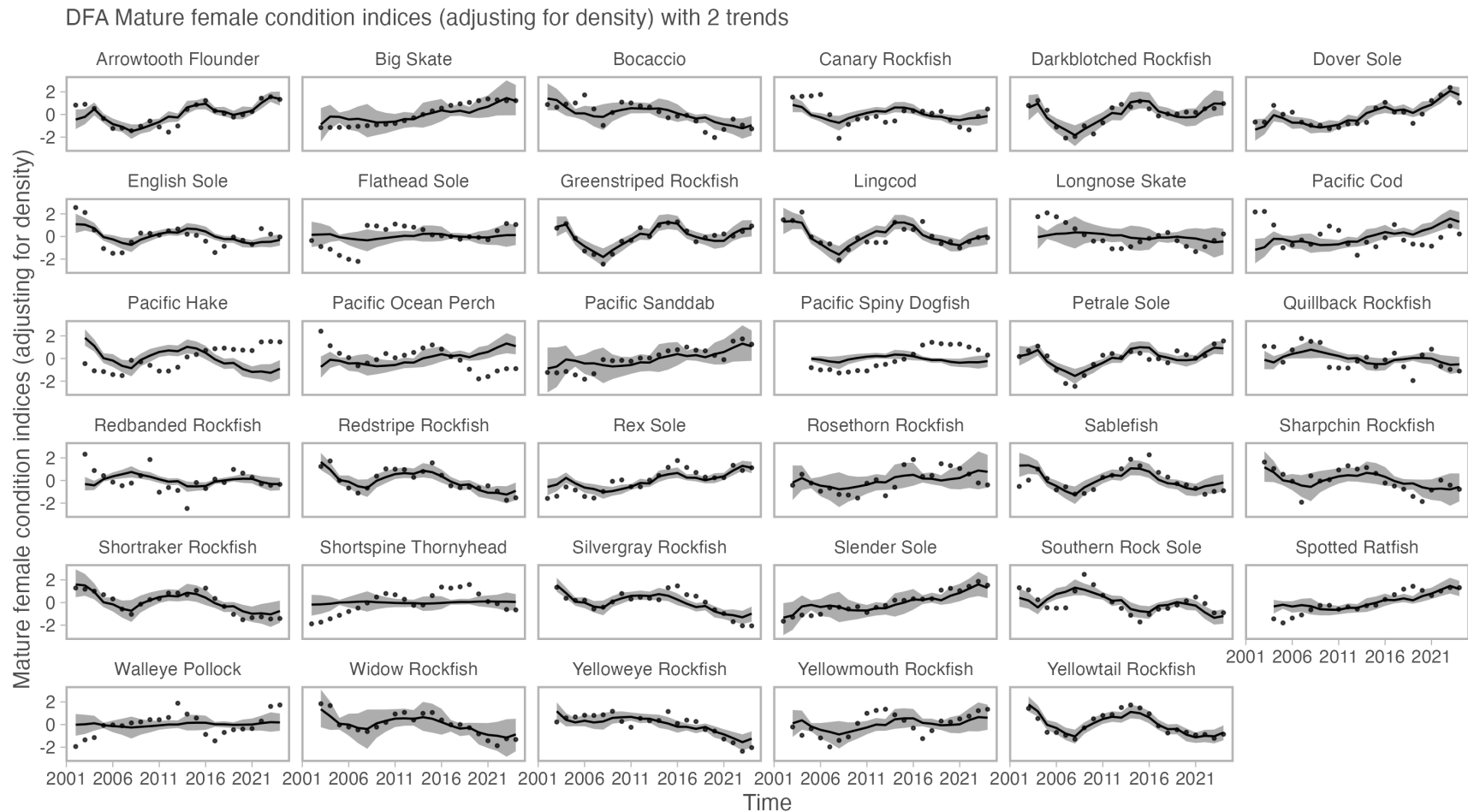


Figure S20: Fit of DFA-derived annual estimates of mature female body condition for each species based on two common trends and species-specific loadings (black line and grey ribbon) and the spatiotemporal model-derived indices of average body condition adjusted for local biomass density (black dots).